RSC Advances

REVIEW

View Article Online
View Journal | View Issue

Cite this: *RSC Adv.*, 2022, **12**, 36073

Dithieno[3,2-*b*:2′,3′-*d*]thiophene (DTT): an emerging heterocyclic building block for future organic electronic materials & functional supramolecular chemistry

Rashid Ali †* and Rafia Siddiqui†

Heterocyclic compounds being potent biochemical materials are ubiquitous molecules in our life. Amongst, the five membered aromatic ring systems, thiophene has emerged as a remarkable entity in organic electronics owing to its (i) high resonance energy, (ii) more electrophilic reactivity than benzene, (iii) high π-electron density, (iv) planar structure and, (v) presence of vacant d-orbital in addition to the presence of loosely bind lone-pairs of electrons on sulfur atoms. In recent past, thiophene-fused molecule namely, dithienothiophene (DTT) has attracted a tremendous attention of the researchers worldwide due to their potential applicability in organic electronics such as in solar cells, electrochromic devices (ECDs), organic field effect transistors (OFETs), organic limiting diodes (OLEDs), fluorescent probes, redox switching and so forth because of their (i) higher charge mobility, (ii) extended π-conjugation, and (iii) better tuning of band gaps, *etc.* In this particular review article, we envisioned to report the recent advancements made on the DTT-based architectures not only because of the potential applicability of this valuable scaffold in organic electronic but also to motivate the young researchers worldwide to look for the challenging opportunities related to this privileged building block in both material sciences and functional supramolecular chemistry.

Received 13th September 2022
Accepted 8th December 2022

DOI: 10.1039/d2ra05768a

rsc.li/rsc-advances

Department of Chemistry, Jamia Millia Islamia, Jamia Nagar, Okhla, New Delhi-110025, India. E-mail: rali1@jmi.ac.in; Tel: +91-7011867613

† Both the authors contributed equally.

Dr Rashid Ali is a pioneering researcher engaged in the area of organic & supramolecular chemistry who earned his PhD from the Indian Institute of Technology, Bombay, at present one of the best institutes in India. He has 12 years of research experience, around one year spent at Sookmyung Women's University, South Korea, and is a holder of more than 50 original research papers published in journals including Nat. Chem., JACS, Chem. Commun., Green Chem., and Coord. Chem. Rev. etc. Currently, he is working as an Assistant Professor in the Department of Chemistry, Jamia Millia Islamia (a Central University), New Delhi, India.

Rafia Siddiqui obtained her bachelor's degree in chemistry from Gargi College, Delhi University in 2015. She completed her post-graduation in organic chemistry from Jamia Hamdard University in 2017. She worked as a project assistant for two years in Department of Chemistry, Jamia Millia Islamia, where which she focused on the area synthetic organic chemistry under the supervision of professors Dr Rashid Ali.

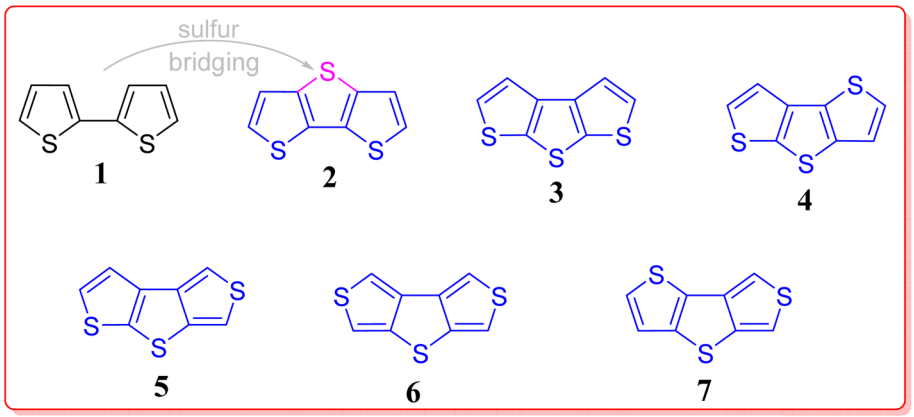

Fig. 1 The structures of 2,2′-bithiophene **1** and five constitutional isomers of DTT (**2**).

1. Introduction

In recent years, polyaromatic hydrocarbons (PAHs) in general and π-conjugated heterocycles in particular have attracted a great attention from researchers worldwide owing to their exceptional applicability in various fields.[1] Generally, heterocyclic compounds are vital molecules as they play a significant role in biochemical fields, pharmaceutical, organic electronics, medicinal chemistry and also in the material sciences and technology *etc.*[2–16] The five membered doubly unsaturated cyclopentadiene system is a non-aromatic, whereas the five membered heterocyclic systems *viz.* furan, pyrrole and thiophene having oxygen, nitrogen and sulfur, respectively are aromatic in nature as the lone pair present on the heteroatom (in unhybridized p-orbital) in these systems participate in conjugation, thereby resulting in the Huckel's aromaticity (cyclic, planar, conjugated, & $(4n + 2)\pi$ electrons). Interestingly, among the thiophene, pyrrole and furan, thiophene has highest resonance energy (29 kcal mol^{-1}) in contrast to the resonance energy of pyrrole (22 kcal mol^{-1}) and furan (16 kcal mol^{-1}). Notably, thiophene display less electrophilic reactivity in comparison to pyrrole and furan but it is more reactive than benzene. Therefore, due to unique characteristics of thiophene in comparison with the other five membered heterocycles, thiophene-based materials have engrossed a tremendous interest of the scientific community around the globe, as they play a critical role in organic electronic and also have substituted the silicon based structures because of their better current on/off ratio and charge transfer mobility.[17] Additionally, the combination of low conductivity (off state), oxidation stability, and the charge transferability ($>1 \times 10^{-3}$ cm^2 V^{-1} s^{-1}), broaden their scope in organic semiconductors. More interestingly, the extensive π-conjugation in the thiophene-based architectures results in reducing the band gap, and hence enhancing the charge carrier mobility which is noteworthy from the semiconducting materials point of view and for photoswitchable system as well. In recent years, fused thiophene systems for instance thienothiophene (two annulated units of thiohpene), DTT (three fused subunits of thiophene), and thienoacenes (more than three annulated units of thiophene) are being found more compatible in tuning the band gap, and display diverse potential applications ranging from the OLEDs, OFETs, solar cells, organic dyes, fluorescent probes, to the chalcogen bonded cascades *etc.*[18–28] Among the fused thiophene systems, dithieno[3,2-*b*:2′,3′-*d*]thiophene **2** and its congeners have fully-fledged due to their inimitable architecture, which can be treated as sulfur atom bridging 2,2′-bithiophenes **1**, consisting one of the sulfur atom (central one) pointing in the opposite direction to that of the other two peripheral ones (Fig. 1). Interestingly, as can be inspected from the same Fig. 1, five more constitutional isomers are possible by permutations and combination of the three sulfur atoms, and a myriad of other heteroatoms could be incorporated into its periphery besides a variety of substituents could be installed in the core structure of DTT. Fascinatingly, DTT (**2**) is an electron rich system having a flat structure, therefore it can nicely intend a number of possible designed materials having stimulating intermolecular interactions (*e.g.*, S···S & π–π-interactions *etc.*), molecular rigidity, self-assemblies, in addition to easy tunable physiochemical properties.[29,30]

In recent years supramolecular interactions also known as non-covalent interactions for instance Lewis acid–base pairing, coulombic attractions, halogen bonding, metal coordination, dipole–anion, π–π-stacking, cation–π, anion–π interactions and other combinations thereof.[31–35] Not surprisingly, the design and synthesis of supramolecular architectures consisting of thiophene subunit(s) – presenting such types of versatile non-covalent interactions will open-up novel opportunities for the research community globally. Keeping the importance of DTT building block in mind, we envisioned to assemble the recent achievements made in this wonderful area of research. Hopefully, this particular review article will encourage new adventures and will surely make a new dimensions in the area of organic electronics as well as in functional supramolecular chemistry.

2. DTT-based molecules and their potential applications

Over the past few years, molecules consisting of the DTT-framework has found a special interest because of their lower

band-gap, excellent electron transport properties in addition to displaying vital supramolecular intermolecular interactions.[36–39] Due to the unique characteristics of the DTT-based molecules *viz.* (i) planar (flat) in nature, (ii) structural rigidity, (iii) π-extended conjugation (iv) easy functionalization, (v) high thermal as well as photochemical stability and so on. Noticeably, various research groups worldwide like, P. Frère,[39] A. B. Holmes,[24,40] T. Ozturk,[30] M. Grätzel,[41] *etc.*, have contributed significantly in highlighting the productivity of the thiophene based systems, specially DTT in the field of electronics. They have shown wide applicability in D–A, D–π–A, D–π–D, (D-donor, A-acceptor), and π-spacer systems for dye sensitized solar cells, organic dyes, polymers and copolymer with acceptor entities, anion transport, catalysis, fluorescent probes, photosystems and anion binding *etc.*[24,39–46] Remarkably, these derivatives on replacing inorganic elements have also endorse environmentally friendly procedures.[47,48]

2.1. DTT-based electrochromic copolymer

Conjugated polymers, being promising materials in the field of organic electronics, have received a great attention in the construction of organic electrochromic (EC) materials[28,49,50] solar cells,[51] OLEDs,[52] & OFETs,[53] *etc.* The organic EC materials on oxidizing electrochemically display reversible color change,[54] short switching timings,[55] and are also highly economic for supplementary production, *viz.* smart sunglasses,[56] *etc.* In this arena of research, pure donor polymers (3,4-dialkoxy substituted thiophenes), conjugated D–A polymers, and non-conjugated triphenylamine (TPA) based polymers have been extensively studied.[57] Interestingly, the non-conjugated TPA and conjugated diketopyrrolopyrrole (DPP) based polymers holds excellent properties *viz.* high thermal as well as film-forming stability, solubility in organic solvents, reversible redox cycles, *etc.* These substances are also highly efficient in hole transport, photoconductors, study of interface engineering, and so on.[58,59] Moreover, the conjugated microporous polymers (CMPs) are easy to functionalize and poses various applications like organic electronics, photovoltaics, sensing and so forth, and it has been noticed that through the incorporation of fused thiophenes into the CMPs enhanced their performances.[60–63] To this context, the research groups of Ozturk & Thomas have constructed DTT-CMPs by means of bulk and electrochemical oxidative polymerization reactions (Scheme 1).[64] During the doping and de-doping process, rapid color change of monomers was observed *via* naked eyes. It was revealed from the spectrochemical measurements that DTT-CMPs, (**10** & **11**), can be

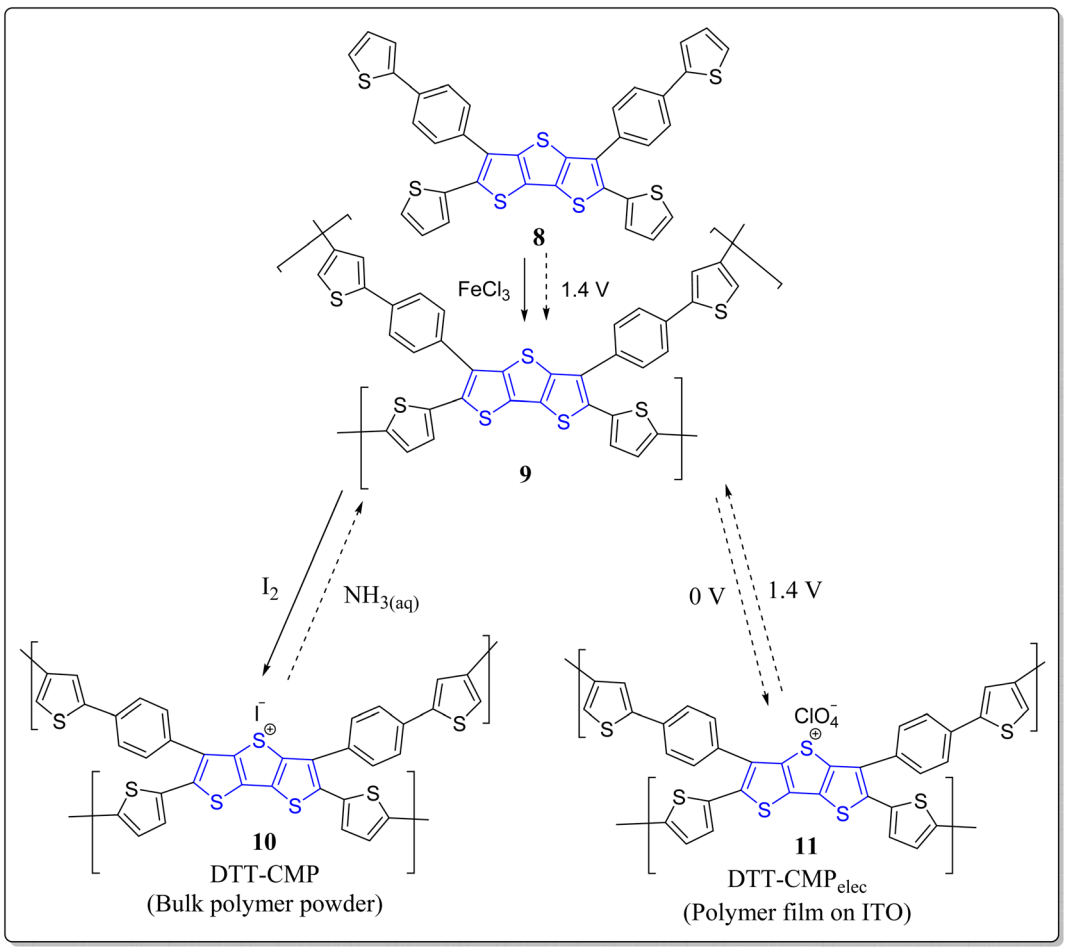

Scheme 1 Designed and construction of the DTT-based polymeric materials **10** and **11**.

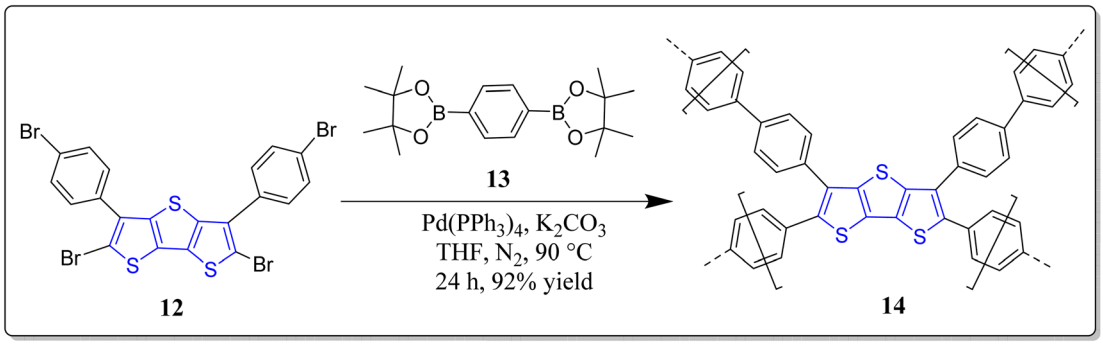

Scheme 2 Synthesis of DTT-CMP (**14**) by means of the Suzuki–Miyaura polycondensation.

reversibly oxidized and reduced, making the systems suitable for electrochromic devices. From nitrogen gas sorption values of the doped, de-doped, and neutral polymer networks, authors analyzed the existence of iodine in the interior pores, and on doping with iodine, the conductivity of the polymeric network increases extensively. This versatile methodology represents the importance of electron rich DTT-moiety in conjugated systems and its applicability in redox switching making DTT-CMPs remarkable materials for both organo-electronic as well as opto-electronic devices in addition to the sensing of ammonia-based explosives.

One year later to the above discussed report, these authors have also revealed a different electron-rich DTT-CMP **14** by treating the DTT derivative **12** with benzenediboronate ester **13** in a Suzuki–Miyaura polycondensation reaction (Scheme 2).[65] They executed the chemical oxidation through iodine exposure which was found to be completely reversible with the treatment of NH_3, monitored by UV-vis and IR spectroscopic technique during the redox process. Interestingly, the property of immediate change in color of the synthesized polymer with the electron acceptors and the polymer oxidized form against the electron donor vapors expands their utility as a sensor to detect ammonia based explosives. Moreover, these types of practices could also be employed to create bulk heterojunctions in porous polymeric materials.

In 2015, Wang *et al.* synthesized the regio-random homopolymers **22a–b** of 3-alkyldithieno[3,2-*b*:2′,3′-*d*]thiophene starting from the 3,4-dibromothiophene **15** as detailed in the

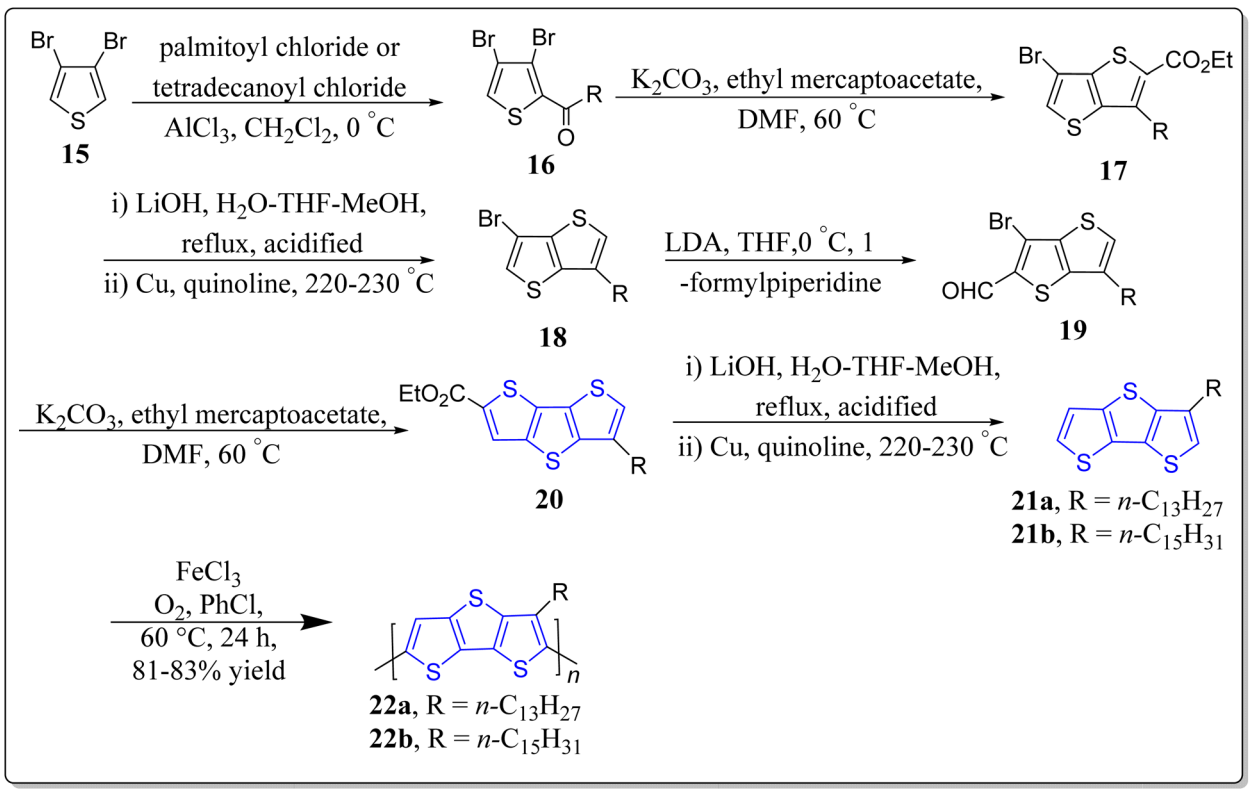

Scheme 3 Design and synthesis of the regio-random homopolymers **22a–b**.

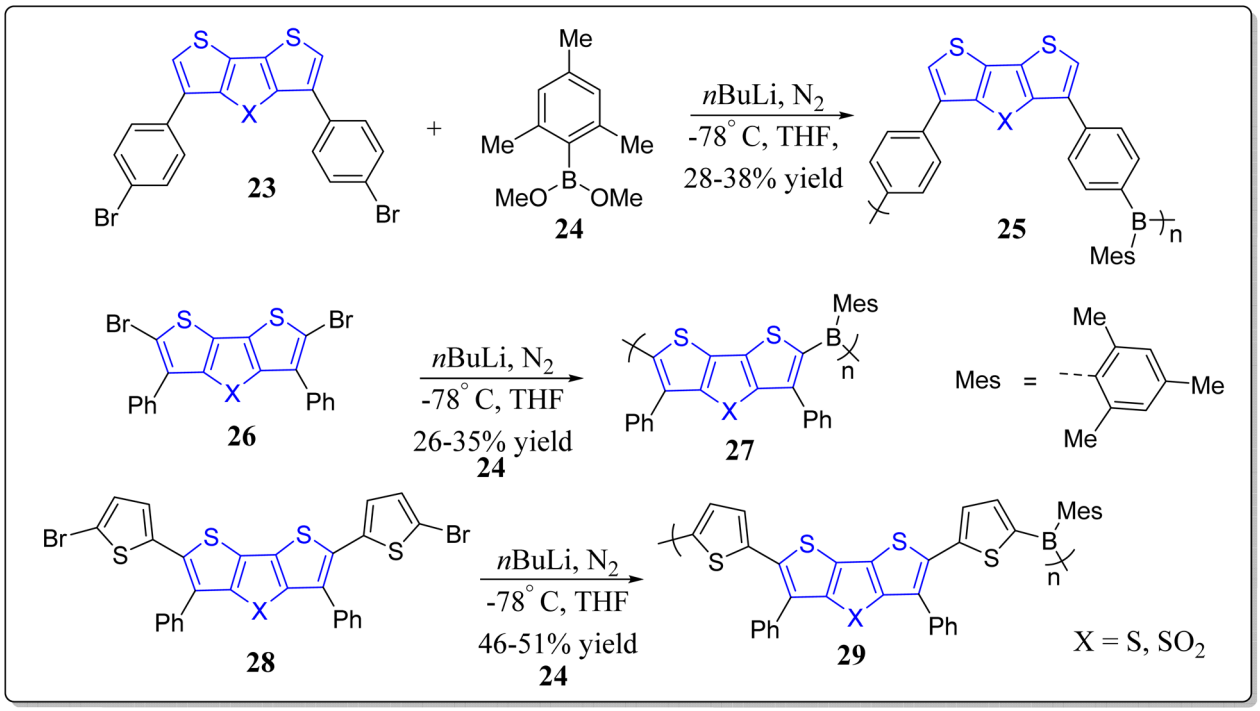

Scheme 4 Construction of the copolymers containing DTT & DTT-*S*,*S*-O_2 units.

Scheme 3.[66] Remarkably, for OFET devices, they showed better self-assembly, oxidative stability, charge mobility (0.048 cm^2 V^{-1} s^{-1}), thermal stability of 0.13 cm^2 V^{-1} s^{-1} at 200 °C, and a current on/off ratio of more than 10^5. Such results promote the scope of utility of DTT in OFET devices.

On the other hand, as can be seen from an inspection of the Scheme 4, DTT-based copolymers possessing mesitylboron moiety in their structures, have been revealed by the group of Ozturk for optoelectronic applications.[67] These authors studied the electrochemical and optical properties of thus formed copolymers, and observed that the polymers with DTT framework display greater band-gap (2.46–3.21 eV) than the polymers synthesized from DTT-*S*,*S*-O_2 (2.18–2.88 eV). Among the all synthesized polymers, **25** exhibits the lowest reduction potential (−1.471 V) and the highest oxidation potential (1.413 V). Additionally, they revealed from the DFT calculations, an intramolecular charge transfer from the donor (DTT) towards the acceptor (boron). From the TD-DFT calculations, they noticed the vertical excitations (HOMO to LUMO) and emissions (LUMO to HUMO).

Moreover, in continuation of the development of DTT-based polymers,[68] the same group has also synthesized bithiazole and DTT-based polymers **39**, **40**, and **41** – exhibiting excellent optical and electronic properties (Scheme 5).[69] In this particular study, the they first synthesized a donor **35** (3,5-dinonyl-2,6-dithiophenyl-DTT), and an acceptor **38** (nonylbithiazole), as shown in Scheme 5. Later on, self electropolymerization of **40** and **43** by virtue of the cyclic voltammetry afforded the polymers **39** and **40** (Scheme 5). Whereas electropolymerization of the monomers **35** and **38** in a ratio of 1 : 1, provided successfully the mixed polymer **41** (Scheme 5). All the synthesized polymers were then characterized by means of the cyclic voltammetry (CV), CV-UV, and UV-vis spectroscopic techniques. Among the synthesized polymers, they observed lowest band-gap for the polymeric material **41** (1.95 eV) in comparison with the **39** (2.17 eV) and **40** (2.53 eV). Next, using spectroelectrochemistry (SEC), the electrochromic properties of thus formed polymer films were inspected. They noticed from these studies, a yellow-orange color for the polymer **39** in its neutral state which turned into the blue-grey with increasing the oxidation level while as **41** in its neutral state exhibited red color which become brown at the intermediate oxidized state and grey at the final oxidized state, displaying that these versatile polymers have multi-colored characteristics. Finally, the electrochemical impedance spectroscopy was employed for the synthesized polymeric films to measure the charge transfer resistances and it was revealed that **41** exhibited the highest current density and lowest resistance in comparison to the other polymer films. To their expectation, the conjugated polymer **41** could found applications as a capacitor besides optoelectronics.

Prompted by a wide applicability of the DTT as well as DPP, Choi and teammates have designed and constructed a series of alternating copolymers possessing these two vital moieties in their structures.[70] The authors prepared the three conjugated polymers **45a–c**, and also investigated the effects of the alkyl side-chains installed in the DTT-core on the device performance (Scheme 6). They noticed that in comparison to the polymers **45a** & **45b**, **45c** showed better results for example high solubility, and mobility in thin film transistor (TFT) (6.88×10^{-2} cm^{-2} V^{-1} s^{-2}), in addition to the excellent power conversion efficiency (PCE). Moreover, the system **45c** with long branched alkyl

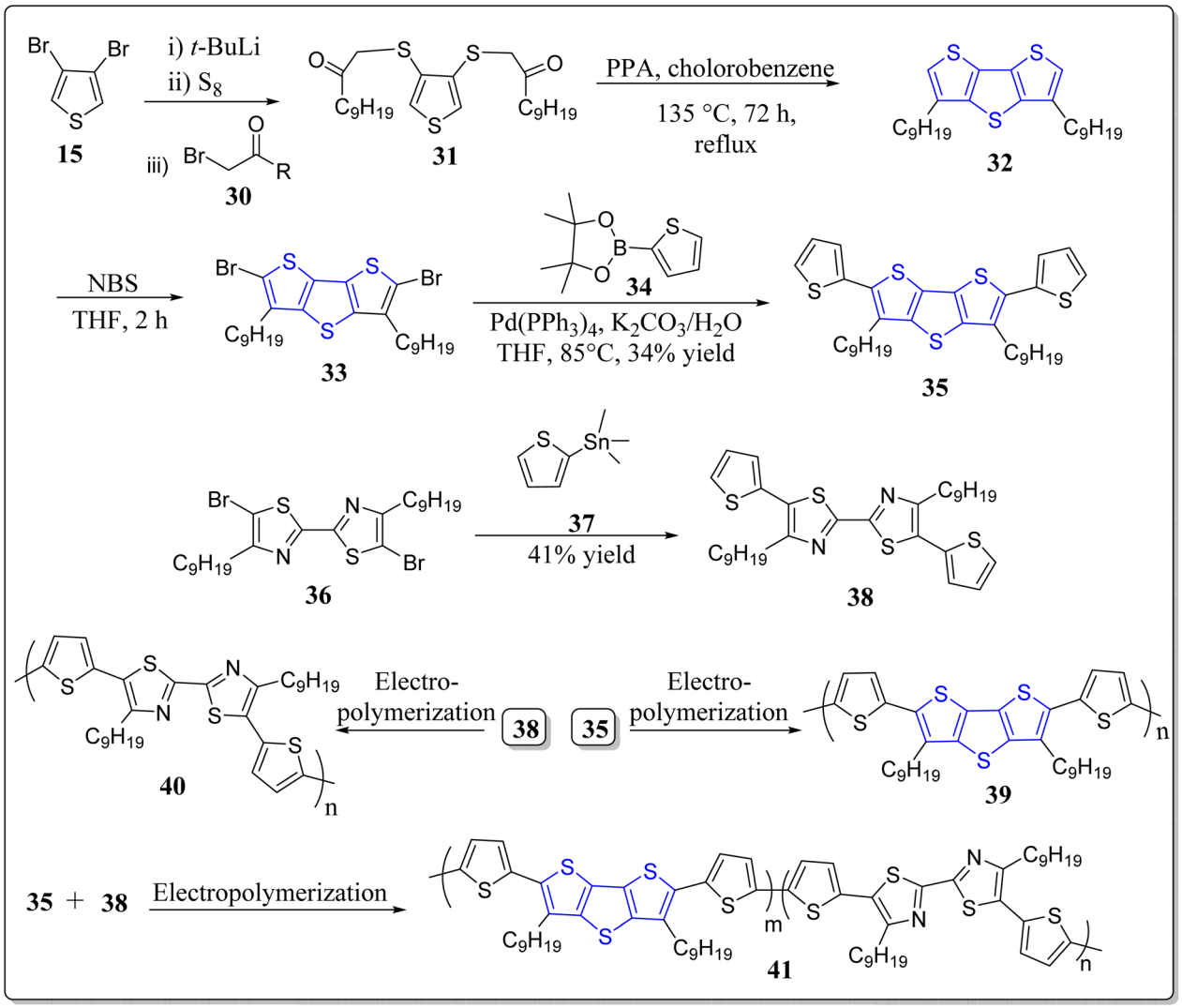

Scheme 5 Electropolymerization of 35, 38, and (35 + 38) to generate the polymers 39, 40 and 41.

chains exhibited great charge transport properties due to strong intermolecular interaction.

In a separate report, Yang *et al.* has revealed the synthesis of a series of conjugated polymers (**50–52**) consisting of DTT as well as DPP subunits in their structures – applicable for the high performance OFETs (Scheme 7).[71] As depicted in the Scheme 7, these systems were assembled by means of the stille polymerization involving the $Pd_2(dba)_3/PPh_3$ in toluene/DMF (10 : 1). Notably, methylated DPP polymers displayed excellent crystalline properties with "face-on" orientation and high mobility for OFETs (5.32 $cm^2 V^{-1} s^{-1}$) in comparison to the non-methylated polymers (5.32 $cm^2 V^{-1} s^{-1}$). These results open-up the opportunities for the installation of other alkyl groups instead of methyl for future OFETs.

On the other hand, the teams of Tajima and Zhou has reported naphthalene diimide (NDI) based n-type photovoltaic copolymers **58a–c** connected to thiophene (T), thienothiophene (TT) and DTT *via* a π-bridge thiophene useful in the fabrication of all-polymer solar cells (Scheme 8).[72] These groups noticed that as copolymerized heteroaromatic rings in the polymers increases, the PCEs of the resulting all-polymer solar cells decreases. Furthermore, they observed distinct molecular orientations for the compound **58a** face-on orientation while as edge-on orientation was found for the polymers **58b** and **58c**.

Tanaka *et al.* has reported a DTT-based conjugated polymer **59** with the incorporation of a furan-flanked DPP which exhibits the high charge transport properties inside the crystalline domains, and the thin film was found to have a low activation energy (<8 meV).[73] The extraordinary transport performance was due to planarity of the backbone of the system **59**, studied by the density functional theory (DFT) calculations. The authors implemented the FI-ESR method for analyzing the intrinsic transport properties of this particular molecule. Moreover, the authors have also explained the interrelation among the charge transport performance and molecular structure.

In a separate event, Lanchao Ma *et al.* devised a novel strategy to construct a conjugated copolymeric nanotube **60** consisting of DTT and perylene diimide (PDI) subunits in its

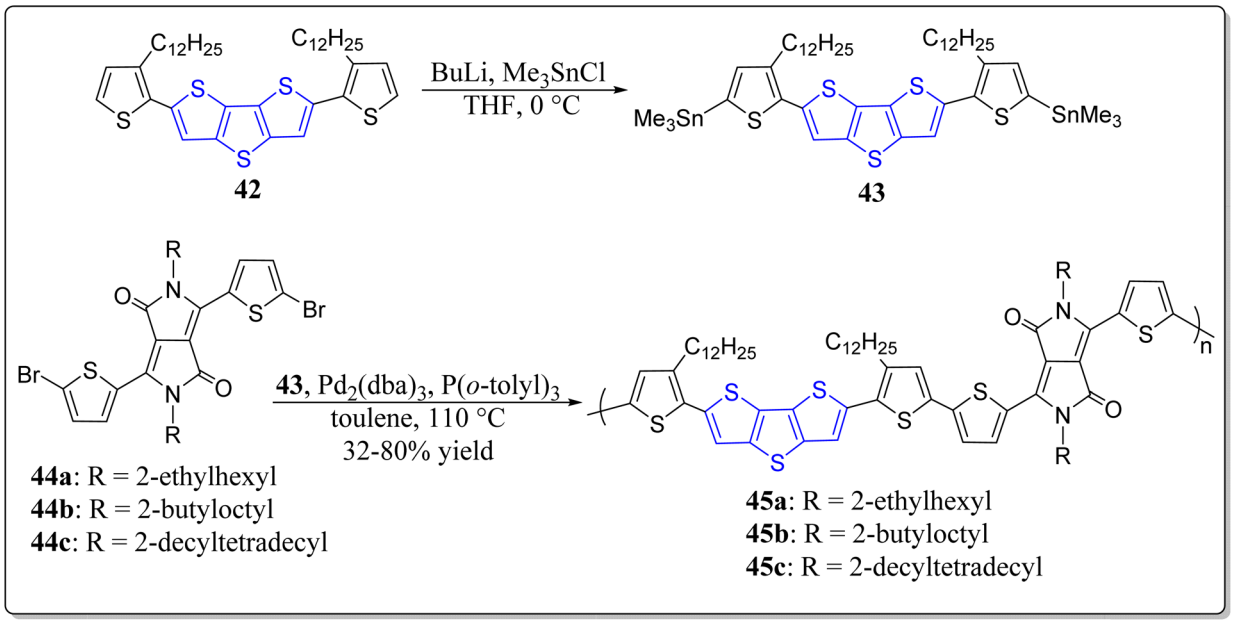

Scheme 6 Synthesis of the DTT-DPP containing conducting polymers.

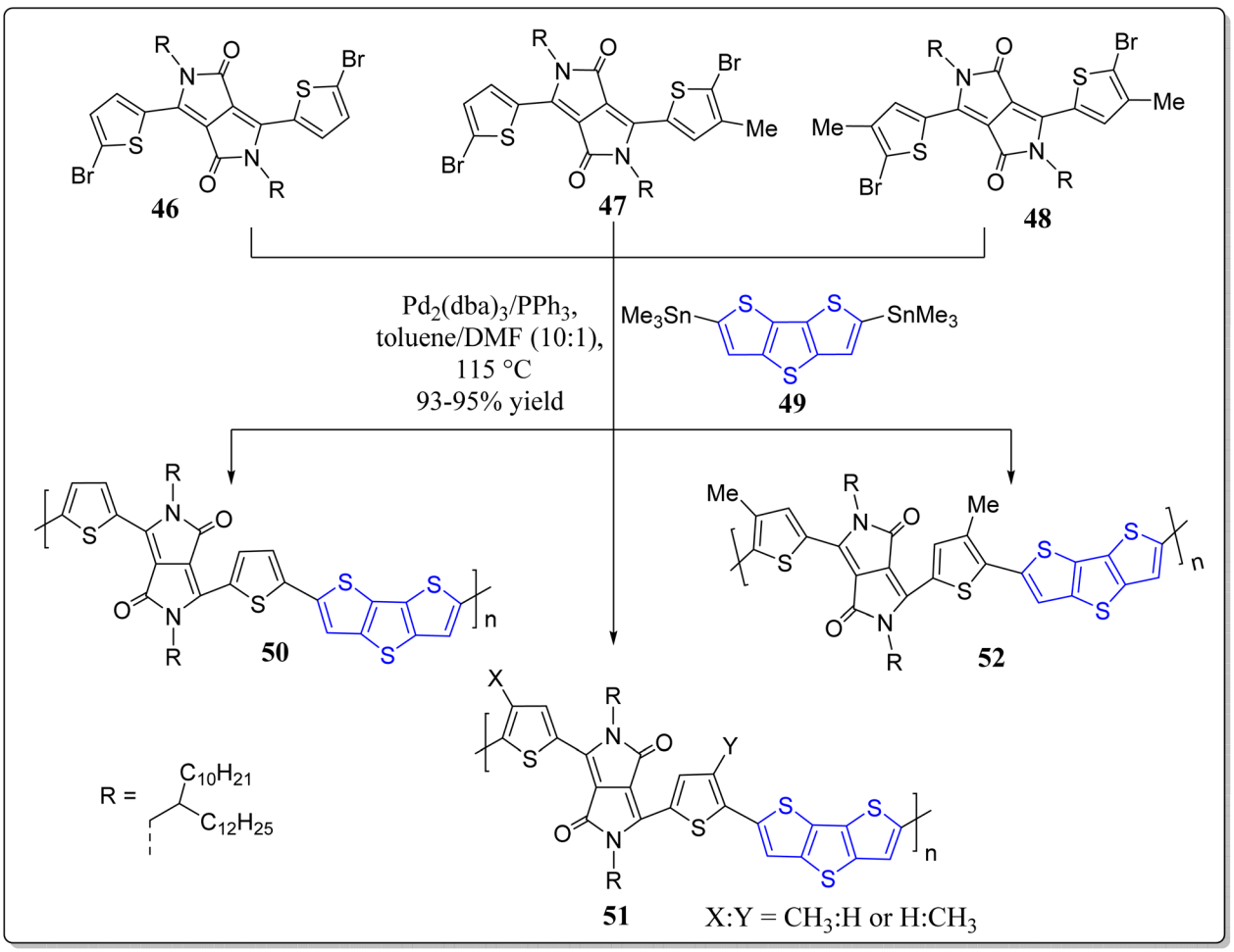

Scheme 7 Construction of the DTT-DPP based polymers **50–52** for field-effect transistors.

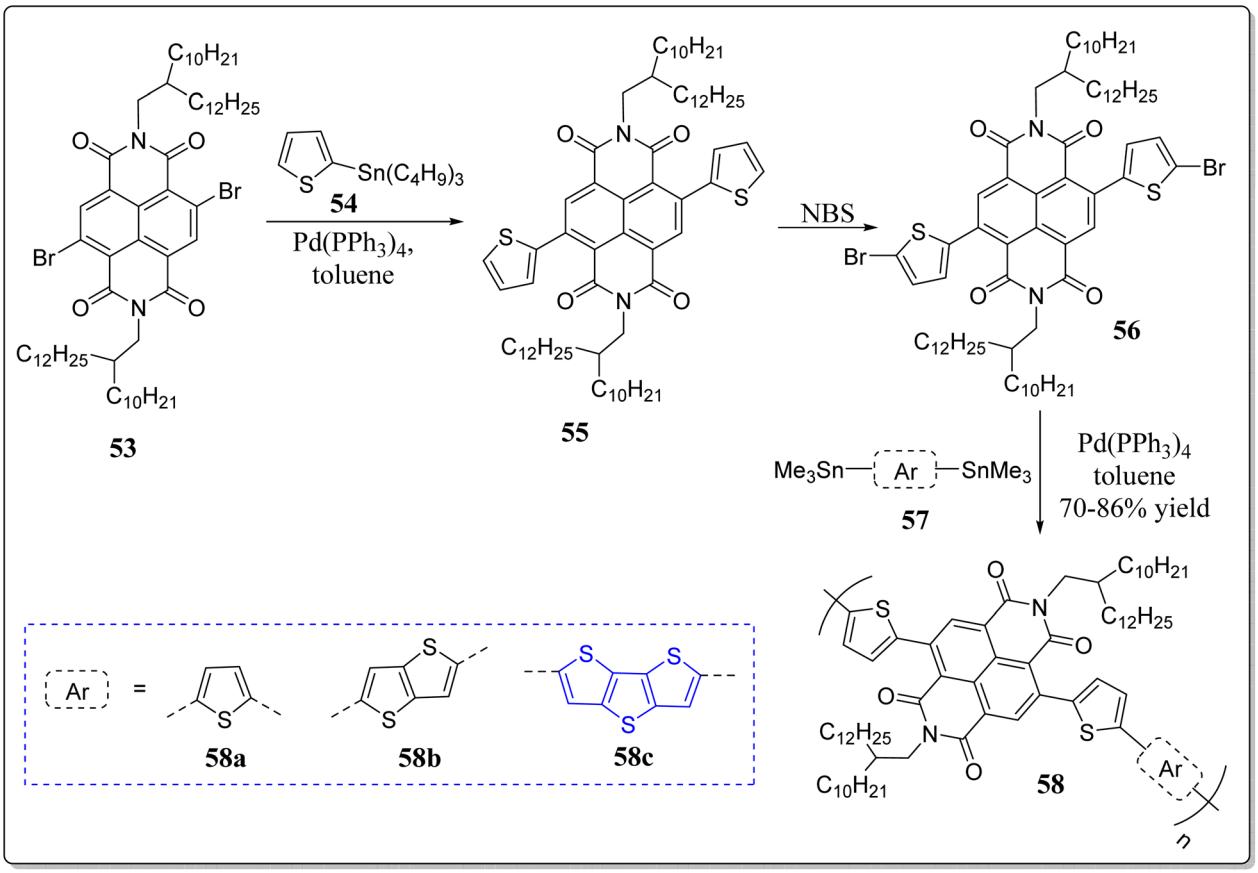

Scheme 8 Synthesis of the copolymers **58a–c** consisting of the bridge thiophene systems.

structure, confirmed through the scanning electron microscopy (SEM) as shown in the Fig. 2.[74] Interestingly, the polymer **60** can be easily synthesized in bulk with regular shape *via* concerned solution and engaging the anodic aluminum oxide template in the solvent medium. Under the ambient condition, in FET, the nanotube exhibited the electron mobility 0.02 $cm^2\ V^{-1}\ s^{-1}$. Furthermore, the nanostructures were fruitfully fabricated by combining the tetraphenylethylene **61** into the polymeric nanotube, forming the light-emitting nano-structures. In a word, the nanotubes **61** have uses for future organic electronics, thanks to the hollow structure & electron transport property.

Polymeric hole-transport layer (HTL) components are vastly employed in the construction of printing technology in perovskite solar cells (PSCs) because of their high solution processability. These materials successfully maintain the mechanical

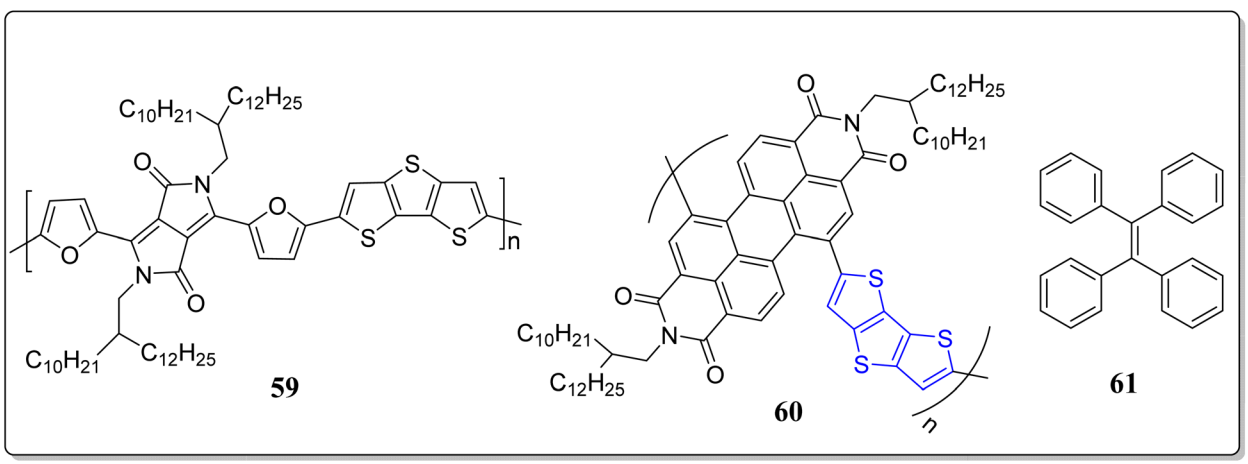

Fig. 2 Chemical structures of the polymeric materials (**59** & **60**) and tetraphenylethylene **61**.

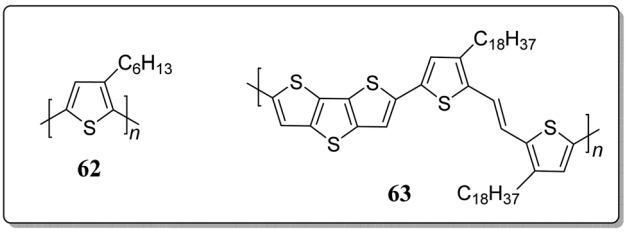

Fig. 3 Chemical structure of the polymeric materials employed for PSCs.

flexibility meant for printing technology. However, these materials have limited carrier mobility, which makes them inadequate for transfer of the charge carriers. Such inadequacy can be eliminated by the incorporation of doping process. On the basis of previous research executed in regard to get a dopant-free HTL substances,[75] recently Jang's research group explored the thiophene unit as an appropriate building block to design a doping-free HTL **63** (Fig. 3).[76] The thiophene unit in the conjugated polymer acting as Lewis base, and can easily coordinate with the Pb^{2+}. In comparison to the reference source of HTL, **62**, which has PCE of 13.9%, the PSCs made-up of **63** exhibited higher PCE of 14.8%. It also showcased a decent performance with 60% under 200 hours having 70–80% of humidity, and advanced hole mobility of 8.03×10^{-4} cm^2 V^{-1} s^{-1}. These results indicate the efficiency of thiophene-based conjugated polymers as a resourceful dopant-free HTL substances.

In another event, Ozturk's research team has designed and constructed the CMP (**66**) consisting of the DTT and triphenylamine *via* Suzuki coupling reaction (Scheme 9).[77] The structural variations of **66** was observed at oxidized and neutral states through FTIR and UV-vis spectroscopy. On applying voltage, the **66** changes its color from orange to blue color. The maximum value of specific capacity and energy density obtained by polymer are, 54 mA h g^{-1} and 43 W h kg^{-1}, respectively at current density of 10 A g^{-1}. Further, the proposed mechanism for polymerization occurs through computational chemistry at two oxidation potentials *i.e.*, 1.2 & 1.5 V, as shown in Fig. 4. Owing to the properties for instance, 60% of optical contrast of CMP, excellent energy storage capacity and easy synthesis makes this polymeric system as a highly potential contender for the electronic applications.

2.2. DTT in sensors

To further extend the earlier work done based on the system **66**, the same group has also synthesized boron substituted

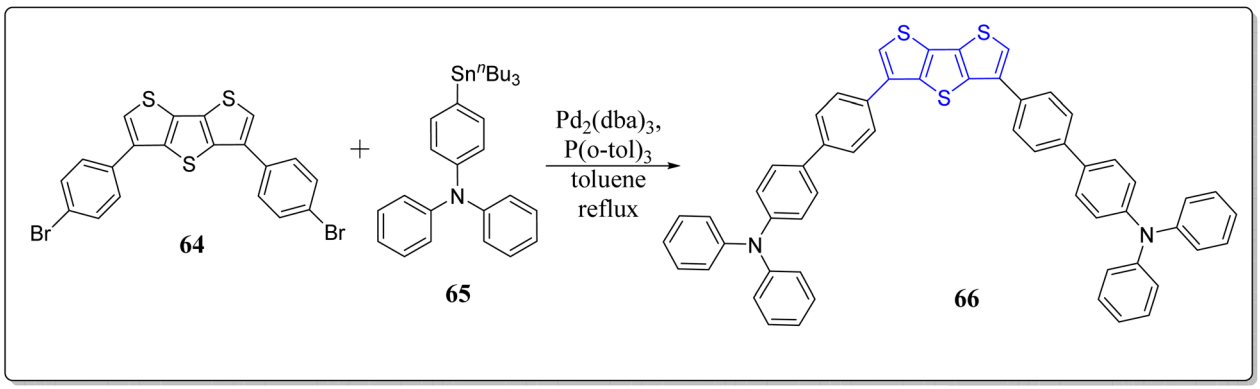

Scheme 9 Designed synthesis of the compound **66** from functionalized DTT and TPA.

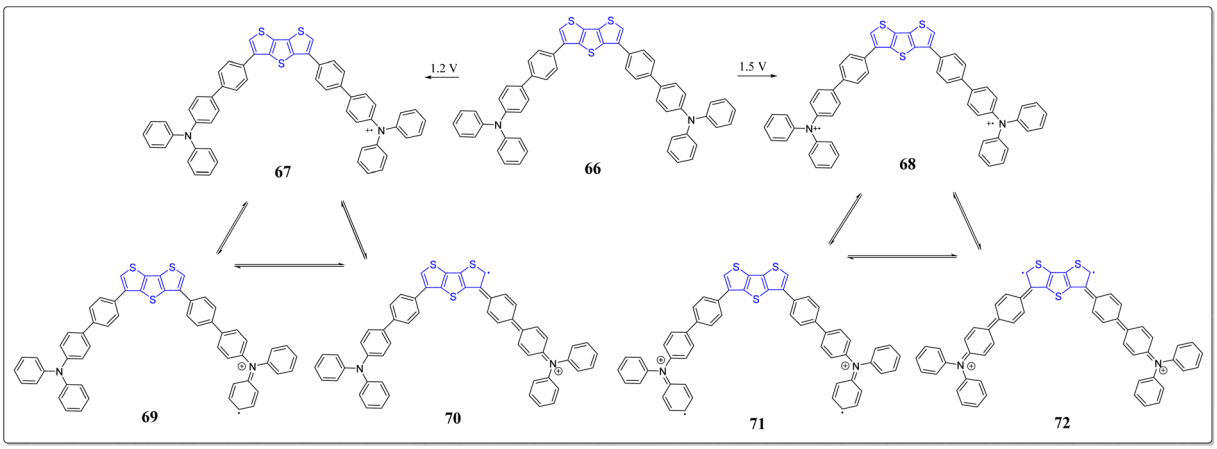

Fig. 4 Electrochemical plausible mechanism of **66** under different voltages (1.2 V & 1.5 V).

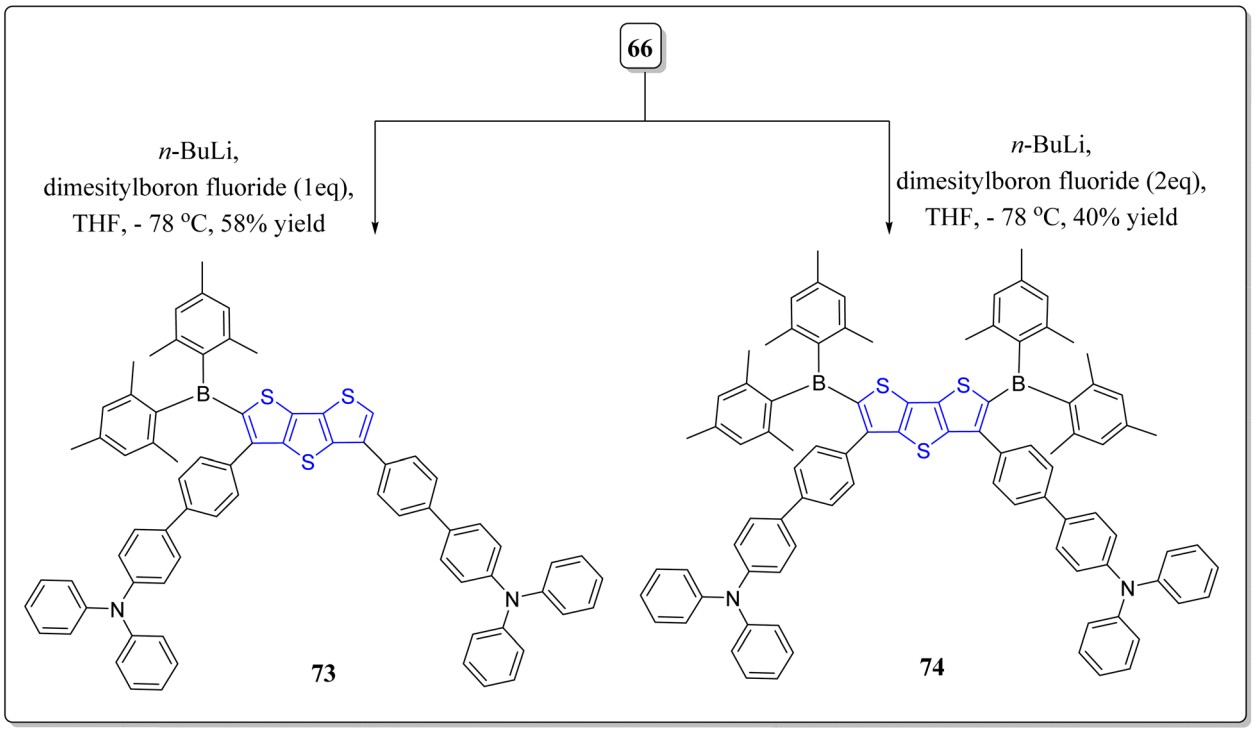

Scheme 10 Construction of the boron-based compound **73** and **74**.

derivatives of **66**, *i.e.*, the compounds **73** & **74**, as shown in the Scheme 10.[78] The solvatochromic investigations of these systems were fruitfully performed, and it was observed that the compound **73** having single boron unit showed more bathochromic shift, moving from the non-polar solvents to the polar solvents. According to the results of fluoride sensing, compound **74** detected more fluoride ions than compound **73** because of the presence of additional boron atom in **74**. Interestingly, the emission sensing limits 23 nM & 25 nM of the compounds **73** and **74**, respectively, and were found the excellent limits reported till date. Additionally, the computational analysis was performed to monitor the flow of electrons from donor to the acceptor (Fig. 5). The importance of thus prepared compounds can be inspected form their incorporation into systems as fluorescent and colorimetric chemosensors.

2.3. DTT in organic solar cells

Organic solar cells (OSCs)[47,79] have productively replaced the utility of inorganic[26] as well as polymeric solar cells, as they are being lightweight, tunable, cost-effective, and reproducible. However, some of the OSCs show limitations because of the low charge transport mobility (LCTM) in addition to the film arrangement. To overcome these limitations researchers globally have synthesized small donor materials with better absorption bands, high charge transport mobility, and good solubility. In this line, quite recently, the group of Iqbal revealed the optoelectronic properties by means of DFT-calculations of three acceptor–donor–acceptor (A–D–A) type molecules (**79–81**) having the DTT-bridge as donor moiety and 2-(3-methyl-4-oxothiazolidin-2-ylidine)malononitrile as an acceptor part (Fig. 6).[45,80] The optoelectronic properties of these novel architectures were compared with the reference molecule **78**, where dithieno(2,3-*b*:3,2-*d*)thiophenes and 2-(3-methyl-5-methylene-4-oxothiazolidin-2-ylidene)malononitrile acting as the donor & acceptor, respectively. From their studies, the authors have noticed the good charge mobility by means of reorganization energies of these versatile molecules. Moreover, the higher value of electron mobility (λ_e) in comparison to the hole mobility (λ_h), showed that thus prepared molecules are best for "hole mobility". From the frontier molecular orbital (FMO), they observed the charge transfer phenomena during the excitation and the molecules indicated relatively low HOMO values along with absorption bands in the range of 459–500 nm, recorded in chloroform solvent. From the electron–hole binding energy studies, they noticed that the molecule **80** possesses the highest number of charges, which may further lead to easy 'dissociation into the separated charges'. Thus, in contrast to **79** and **81**, molecule **80** holds better charge dissociation energy, whereby the highest open circuit voltage (V_{oc}) was found for **81**. Finally, they concluded that the donor molecules (**79–81**), especially **80**, hold auspicious optoelectronic properties – and are useful donor functional materials for the usage in OSCs.

In stark contrast, to improve the performance of PSCs, Liu & Zhang have revealed the hole transporting materials (HTMs) on the modulation of electron deficient π-bridge moieties in the triphenylamine derivatives.[81] They reported a class of donor–π–donor (D–π–D) types of materials (**82a–d**) consisting of 4-methoxy-*N*-(4-methoxyphenyl)-*N*-phenylbenzenamine (MeTPA) as electron rich arms and employed different electron deficient moieties as the bridge (Fig. 7). The authors confirmed the

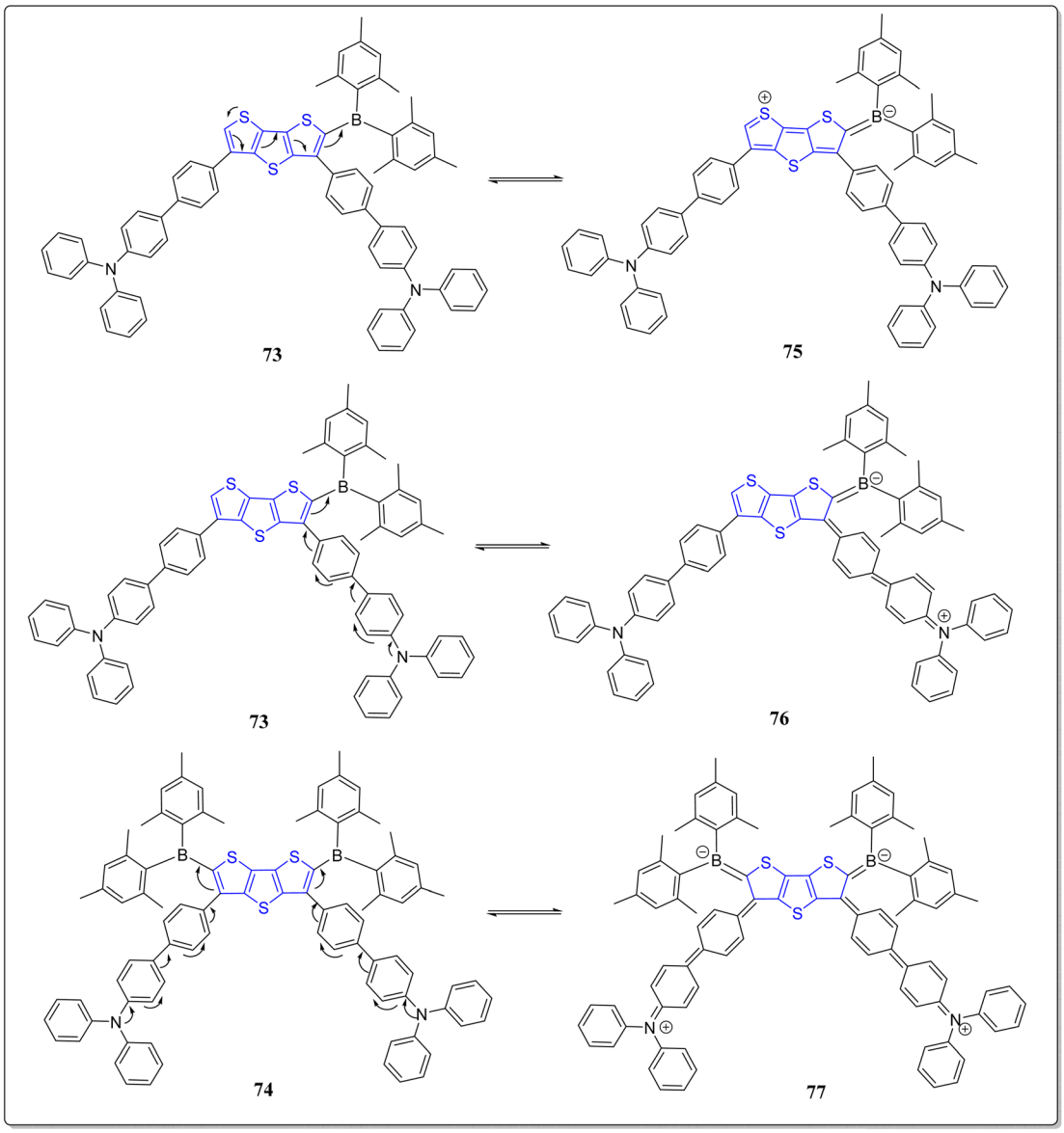

Fig. 5 Schematic representation of electron transfer flow from D–A in the compound **73** & **74**.

superiority of the DTT as a valuable building block through the investigation of fused thiophenes in the application of HTMs and PSCs. Based on the performance of thus designed molecules, various properties *viz.* reorganization energies, geometric structures, hole mobility, electron coupling, stability, solubility, optical absorption as well as the emission were nicely investigated *via* DFT and Marcus theory. Noticeably, among the designed molecules, highest mobility was exhibited by the system **82c** (2.70×10^{-1} cm^2 V^{-1} s^{-1}), consisting of a DTT as a bridge.

In recent years, as the field of OSCs/organic photovoltaics (OPVs) has gained much interest because of their feasible, economical and adjustable electrical and/or optical features.[82,83] To this context, the effect of π-linkers on OPV molecules was revealed by the Hong and Jang's research groups by synthesizing two push–pull D–π–A molecules (**83** & **84**) having almost similar HOMO–LUMO energy levels & band-gaps, for the solution-processed bulk heterojunction OPV devices (Fig. 8).[84] From their studies, they found that the π-linkers in **83** & **84**, play a crucial role in thermal, electrochemical, and thin film morphology. They have incorporated the π-linkers *viz.* triphenylamine and dicyanomethylene-appended indanone as a donor and an acceptor, respectively. From the photovoltaic studies it was observed that the minor variation in the acceptor/donor ratio alters the V_{oc} values of **83**. They further investigated by keeping in mind the active layer thickness, where they noted PCE, V_{oc}, and J_{sc}, values gets decreased on the reduction of the active layer thickness. Thus, in order to have a optimized OPV system, morphology and active layer thickness both should be taken into the account. To get insight of effect of the π-linker on morphology, thermal annealing experiment was carried out, which demonstrated that the roughness of the thin film of **83**

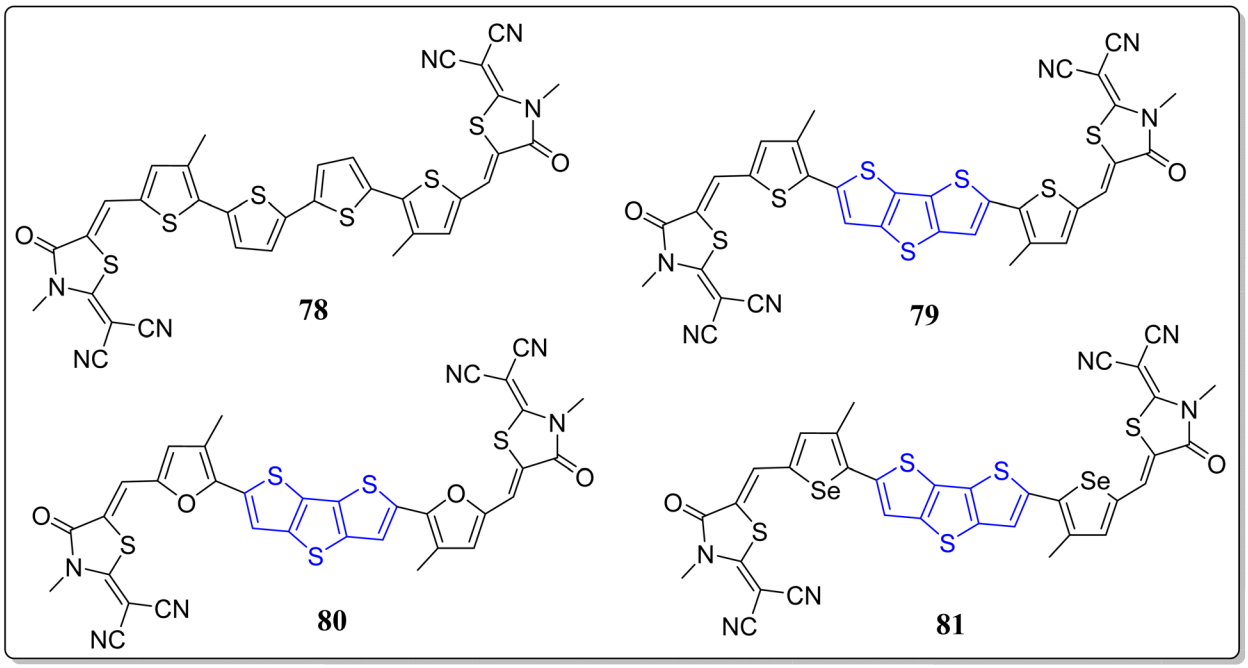

Fig. 6 Structures of the designed (A–D–A) molecules **79–81** along with reference compound **78**.

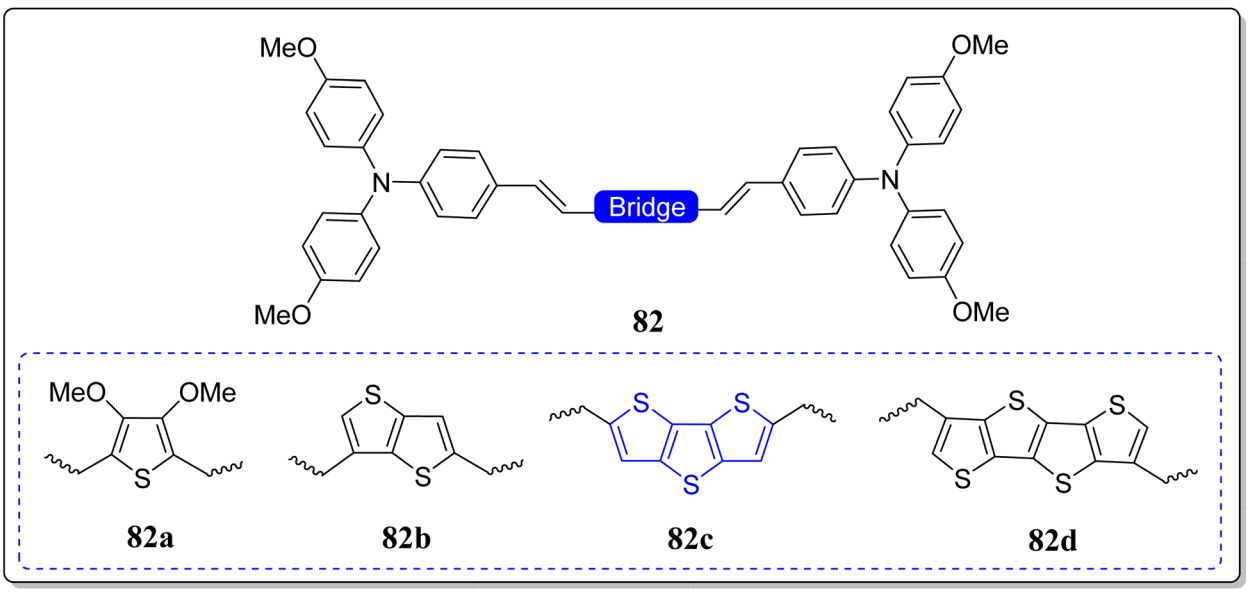

Fig. 7 Chemical structures of the HTMs exposed by the Liu and Zhang.

reduces to 0.235 nm from 0.448 nm. Also, the PCE increased to 2.38% from 1.81%, whereas PCE value decreased in case of **84**. Next, they also found that DTT-based system **83** displayed the high thermal stability in the solid state with well-organized nano-structure morphology, while as **84** showed the excellent electrochemical stability with the faster electrode reaction rate. Finally, they concluded that the decorative design of the π-linkers may be measured for the enlargement of high performance push–pull structure based OPV devices.

On the other hand, in another event, the same group has also fruitfully reported three organic photodetectors (OPDs) **85–87**, having excellent broad band, external quantum efficiency (EQE) (64%, at 530 nm), low dark current density (J_d) (1.8×10^{-8}), and good photocurrent density (J_{ph}) (9.6×10^{-3} A cm^{-2} at −3 V bias).[85] The idea was to discover a strategy to accomplish the lower value of J_d and higher value of the EQE in organic photovoltaics with the aid of π-linked structure of D–π–A push–pull type materials (Fig. 8). From their extensive studies, the

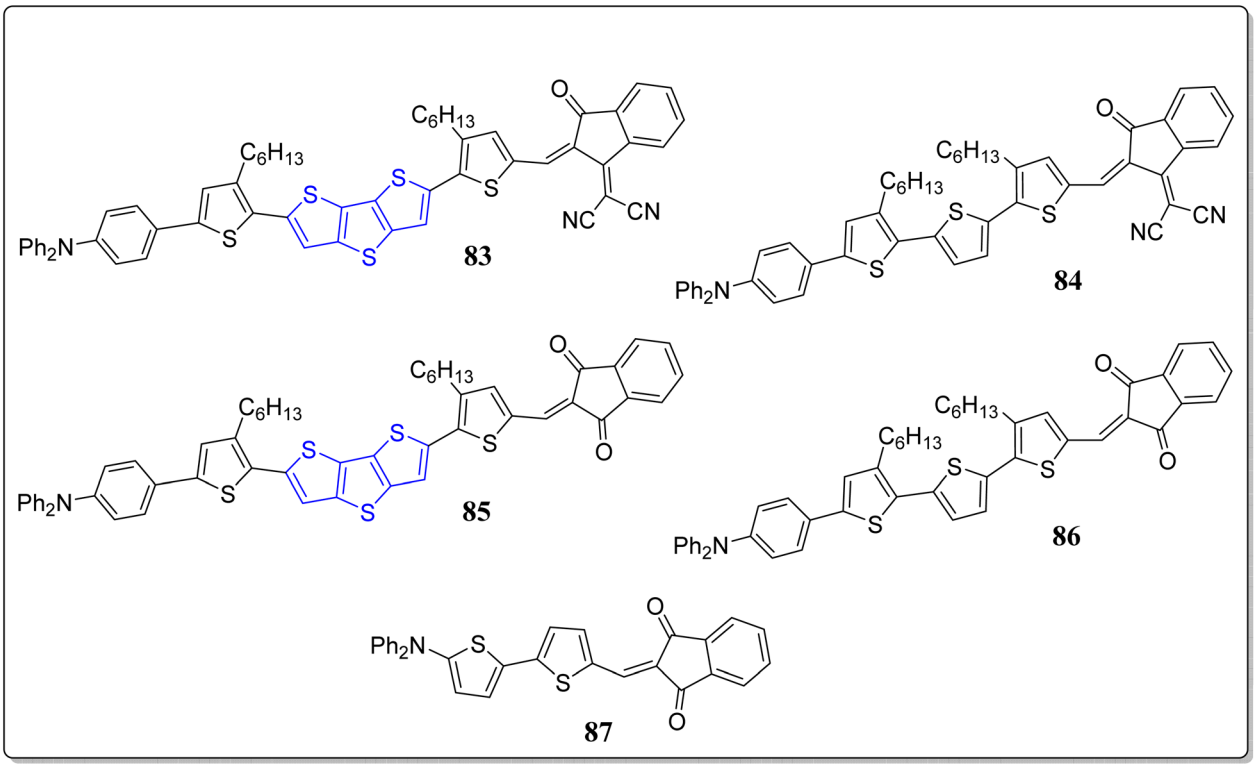

Fig. 8 Chemical structures of the push–pull D–π–A molecules for the OPVs and OPDs.

authors noted down that the stronger intermolecular interactions was found in donor molecule **86**, and forming a polycrystalline structure, hence generating the sub-gap states & trap sites at the interface. And increased the J_d value of OPDs due to facilitated electron injection from indium tin oxide (ITO) electrode to the donor molecule at the reverse bias & decreased the J_{ph} value. In stark contrast, the donor compound **87** having a small π-linker exhibited amorphous morphology in thin films due to weaker intermolecular interactions – lowering the J_d value in both planar heterojunction OPDs & bulk heterojunction OPDs. Remarkably, the developed strategy might open-up new possibilities for designing of novel donor molecules applicable to the valued high performance OPD devices.

2.4. DTT-based cyclic tetramer of selenide

Owing to the fundamental scientific interest, cyclic oligothiophenes has extensively been studied in recent past. However, not considerable work had been reported on the 3-D oligothiophene based architectures.[86] To exploit the work on thiacalix[*n*]dithienothiophene (**90**),[87] Hasegawa and teammates have reported the synthesis of selenacalix[4]dithienothiophene (selenacalix[4]DTT) (**89b**).[88] Keeping in mind the drawbacks of the previously reported methods,[89] these authors have carried out the synthetic strategy *via* one-pot Pd-catalyzed coupling reaction containing silicon atoms, linking the cyclic tetramer of DTT, as shown in Scheme 11. The Se atom posing large van der Waals radius easily forms a 3-D well-arranged network and

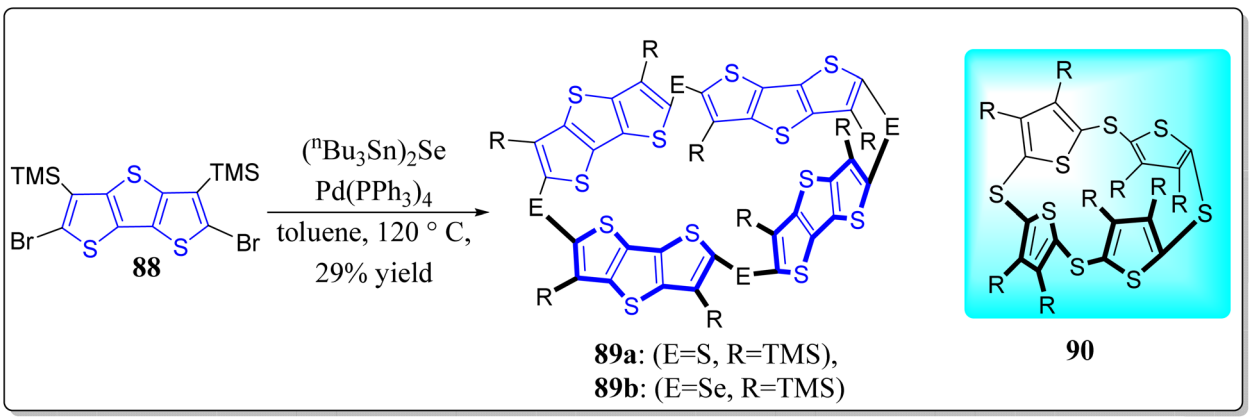

Scheme 11 Synthesis of cyclic DTT system **89** & structure of thiacalix[*n*]dithienothiophene (**90**).

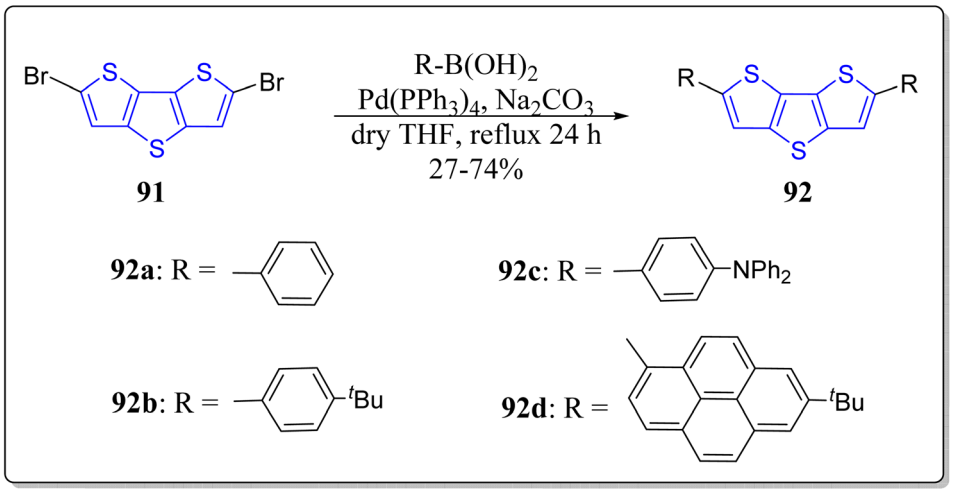

Scheme 12 Designed synthesis of D–π–D monomers *via* Suzuki coupling reaction.

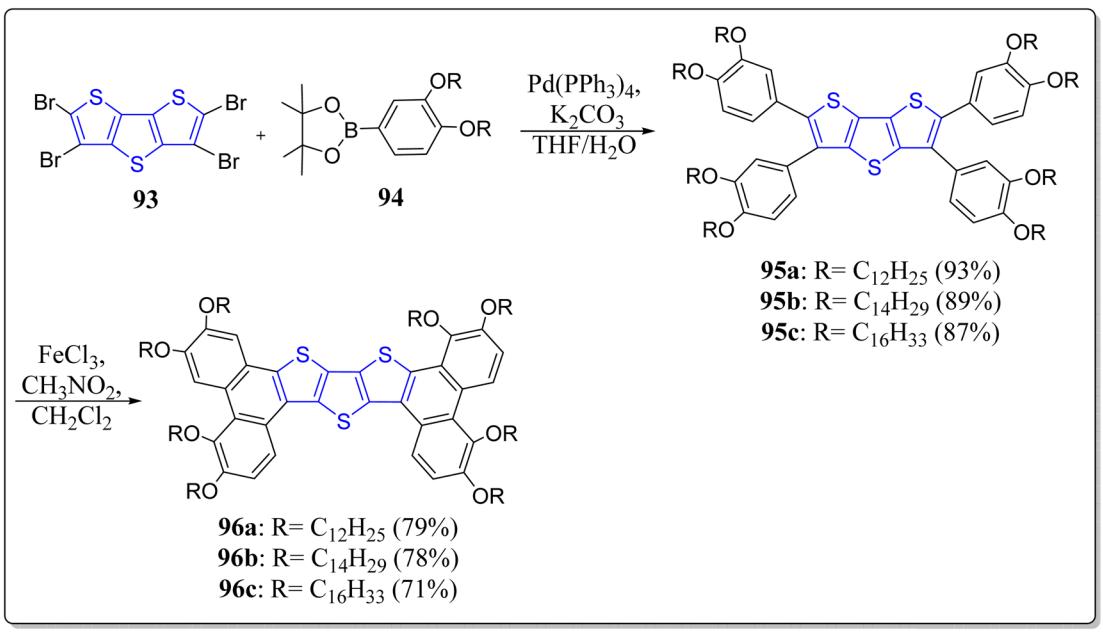

Scheme 13 Schematic representation for the preparation of the DTT-based mesogens.

conducts (i) electron/hole transporting material, (ii) vast host cavity, (iii) increases electron donating ability of DTT, and (iv) setup the molecular assembled porous materials. From the X-ray diffraction studies, it was uncovered that due to Se⋯π interactions, the supramolecular structure turns into the non-planar quadrilateral shape having S_4-symmetry in addition to the cavity along the *X*-axis posing channel like columnar assembly. Moreover, they investigated that the tetrameric system forms a 1 : 2 complex with C_{60} in the solid state, thereby generating the symmetrical 3-D arrangement of C_{60}.

2.5. D–π–D monomers consisting of DTT-scaffold

To explore the potential applications of DTT-based systems in organic light-emitting diodes,[90–92] Matsumoto's research group has synthesized four highly fluorescent blue light emitting D–π–D monomers **92a–c** by virtue of Suzuki–Miyaura cross-coupling reaction as a key step. The authors have studied these versatile chromophores both in solid as well as solution state through UV-vis absorption and fluorescence spectroscopic means (Scheme 12).[93] Fascinatingly, they noticed that incorporation of the aryl groups extends the conjugation and reduce the HOMO–LUMO gap of the thiophene chromophore, thereby red-shift in the wavelength of both absorption as well as emission. The remarkable optical signatures of their solid state powders also unveiled a discrete red-shift than the emissions of their dilute solutions. Notably, close face-to-face π-stacking interactions amongst the DTT molecules was also found to be inhibited, hence improves the fluorescence quantum yields, solubility, and thermal stability of the molecules. The optical

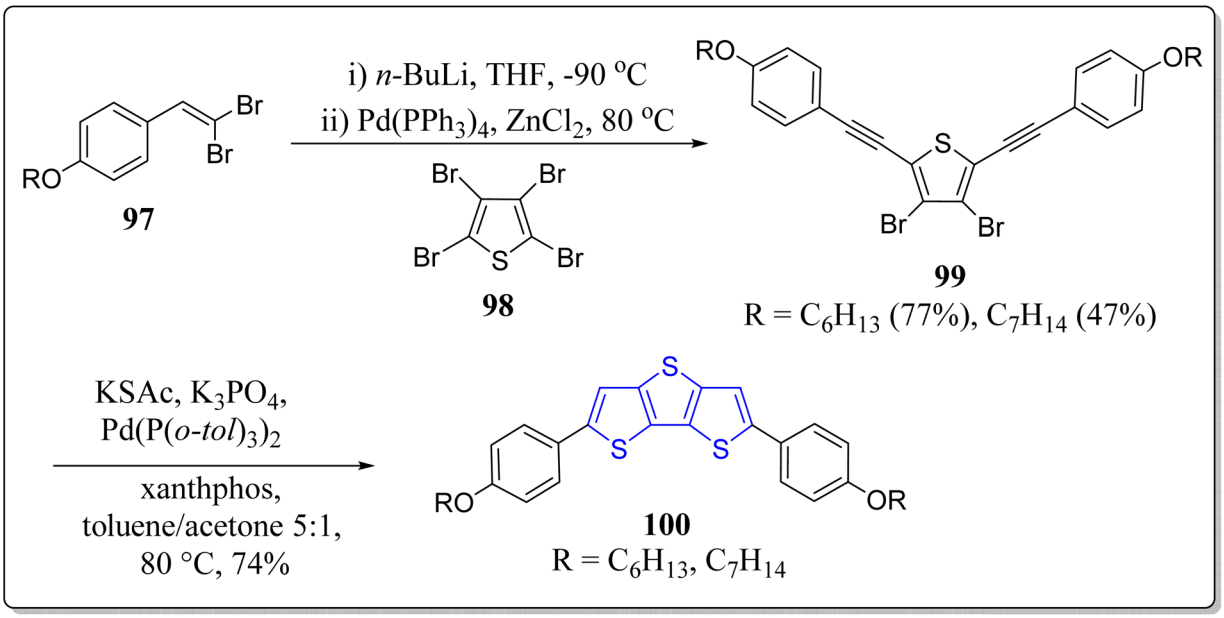

Scheme 14 Design and construction of DTT-derived liquid crystalline dithienothiophenes.

properties of the molecules are primarily affected by the intramolecular charge transfer (ICT) of the D–π–D structures. Among the four synthesized monomers, the increased order of bathochromic shift was observed in the order of **92a** < **92b** < **92c** < **92d.** The energy band-gaps of D–π–D monomers has been calculated by DFT calculations at the B3LYP/6-31G* to prove the

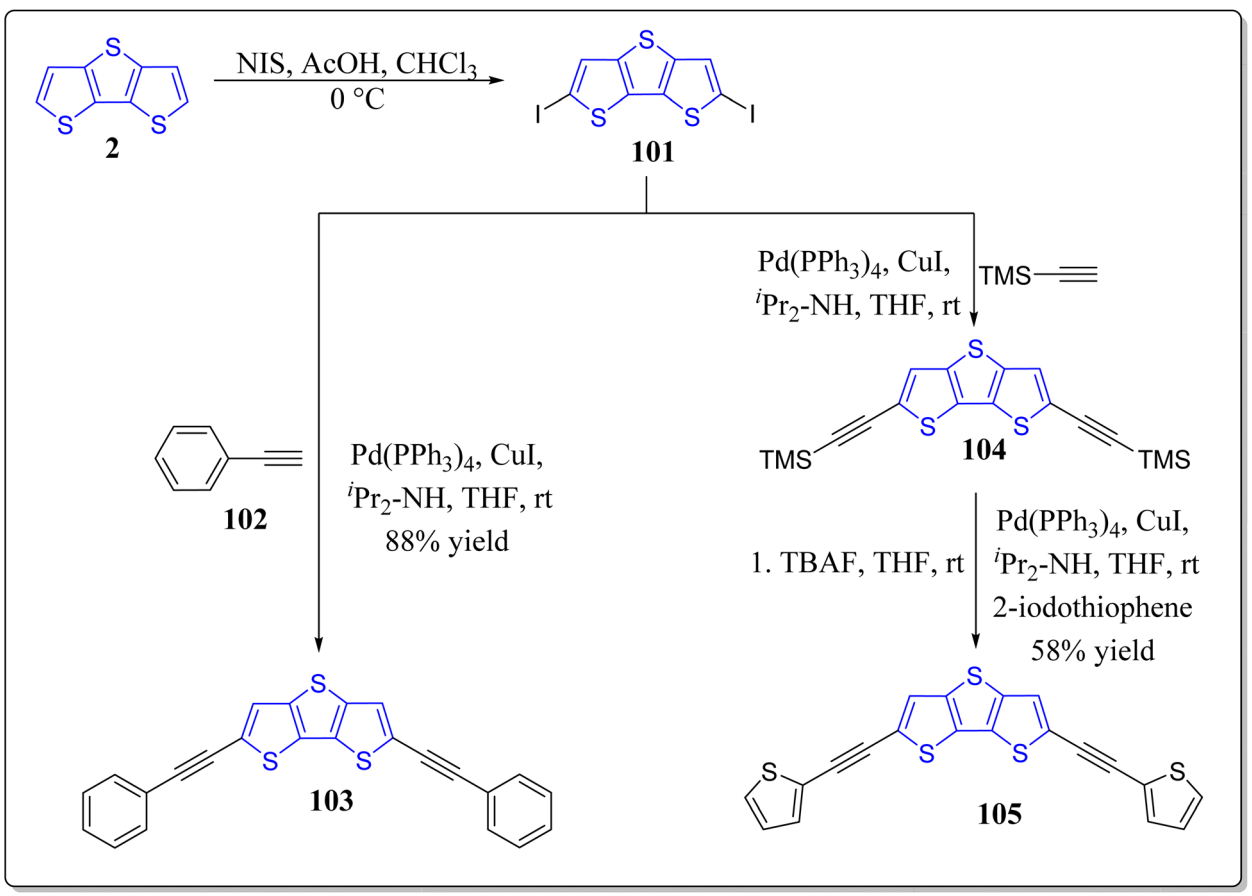

Scheme 15 Synthetic route to afford solution-processable compounds **103** & **105**.

π-extended conjugation of the DTT after the installation of various donor moieties. Finally, they also commented that this tactic could be used to produce diversified highly promising candidates in the fabrication of organic electroluminescence devices.

2.6. DTT-based mesogens

Interestingly, over the last decade, DTT-based mesogen molecules have displayed exceptional charge mobility, hence they have been exploited on a large scale in organic electronics.[94] In this context, Donnio, Monobe & Zhao's groups have designed and constructed the DTT-based sanidic (board-like) liquid-crystalline semiconductors (**96a–c**) in a two-steps tactic involving the Suzuki–Miyaura coupling reaction followed by $FeCl_3$-mediated oxidative coupling as the crucial steps (Scheme 13).[95] The authors have studied their optical, thermal, semiconducting, and self-assembly features. These monomeric molecules displayed the following properties: (i) forms blue-light emitting gels, whose reminiscent of the columnar structure, fibrillary-like morphology, & stabilized through the intermolecular interactions, was confirmed by means of scanning electron microscope (ii) mesomorphic properties, (iii) gets self-assembled into the columnar hexagonal mesophases as established by the differential scanning calorimetry (DSC), polarized optical microscopy, and small angle X-ray scattering analysis, (iv) showed long-lasting blue photoluminescence with quantum yield (33%), and (v) excellent hole transportability with charge carrier mobility in 10^{-3} cm^2 V^{-1} s^{-1} (measured using time-of-flight transient photocurrent technique). Such compounds endorse a good scope for the future DTT-based mesogens.

2.7. Liquid crystallinity in DTT-based molecules

Vollbrecht *et al.* has successfully synthesized two substituted DTT-based semiconductors **95** *via* carbon-sulfur cross coupling reaction and 5-*endo*-dig-cyclization (Scheme 14).[96] At high temperatures, thus made molecules displayed the nematic liquid crystalline behavior. The spectroscopic studies revealed that the HOMO–LUMO energy gap of the these versatile compounds **100** are analogous to the energies of the hole transporter like *N*,*N*′-bis(3-methylphenyl)-*N*,*N*′-diphenylbenzidine (TPD). Moreover, these molecules, in thin-film transistors, exhibited the charge carrier mobilities at 0.03 cm^2 V^{-1} s^{-1} and 0.13 cm^2 V^{-1} s^{-1}. Finally, the inverter circuits in single-type thin-film transistors technology were also implemented by these authors.

2.8. Utility of DTT-based systems in thin film transistors

In recent years, solution-processable organic semiconductors has engrossed a tremendous attention of the scientific community worldwide for the next generation bendable electronic devices in particular OTFTs & OPVs because of their unique assets for instance low cost, solution-processability, light weight, easy fabrication, and compatibility with a large-scale flexible substrates. In this context, innumerable hetero(-aromatic) based entities (*e.g.* thiophene, benzene, & fluorine, *etc.*) with proper substitution have successfully been used to nicely design the novel organic semiconductors with high solution processability and optimal charge transport characteristics. Particularly, solution-processed π-conjugated systems have surfaced for its handy molecular structure, easy synthesis, simple purification, decent yields, & minimal batch-to-batch discrepancy, in comparison to the polymeric counterparts. Amongst the various versatile moieties for the organic semiconductors, DTT is one of the greatly awaited smart materials to be explored for the OTFTs applications. Bearing the importance of DTT-based architectures in mind, in 2018, the research group of Seo constructed and fully characterized the DTT-based solution-processable OTFTs *viz.* **103** (2,6-bis(phenylethynyl) dithieno[3,2-*b*:2′,3′-*d*]thiophene), **105** (2,6-bis(thiophen-2-ylethynyl)dithieno[3,2-*b*:2′,3′-*d*]thiophene) besides the investigation of their optical, thermal & electrochemical properties (Scheme 15).[97] The solution-sheared thin films of these material demonstrated the p-channel properties as an active layer in OTFTs and also exhibited the micrometer-sized crystalline fiber structures. Among the constructed molecules, **103** showed high hole mobility (0.32 cm^2 V^{-1} s^{-1}). Complementary-like inverters were made-up based on the two duplicate ambipolar transistors – resulting in the moderate voltage gains (up to 16).

Encouraged by the usefulness of the asymmetrically substituted DTT-based systems,[98,99] Seo's research group has also successfully reported the solution-processable asymmetrically substituted DTT derivatives **109** as depicted in the Scheme 16.[100] Diverse physiochemical properties like, decomposition temperature, maximum absorption wavelength, HOMO/LUMO, band gap and melting temperature were examined for the operation as organic semiconductors for thin-film transistors. In their studies, all the functionalized DTT-based materials demonstrated the p-channel activity, and the compound **109** (R = octyl) displayed best performance having the hole mobility of 0.07 cm^2 V^{-1} s^{-1}, & at ambient conditions, the ratio of current on/off was greater than 10^8. Furthermore, morphology & the film microstructure displayed the correlation with the corresponding electrical performance, where terrace-like morphology & the high film texture provided the high device performance. On the other hand, in a separate report, the same group has also revealed the synthesis of symmetrically substituted DTT-based organic semiconductors **110** & **113** for thin-film transistors (Scheme 17).[101] It was observed by the authors that all the molecules displayed good thermal stability over 290 °C, different side chains of DTT-based systems provided the different melting temperatures. The energy levels of the molecular orbitals were not only investigated by means of theoretical studies but also experimentally as well, and they found almost same trend. The developed systems were engaged as active layers for top-contact/bottom-gate OFETs with average charge carrier mobility 0.10 cm^2 V^{-1} s^{-1} and the current on/off ratio greater than 10^7 at the ambient atmosphere. Importantly from their studies, the authors observed that DTT derivative having octyl chain in its structure exhibited the best device performance and the high device performance may be ascribed to the large grains & continuous surface coverages besides the high film texture of the analogous semiconductor films.

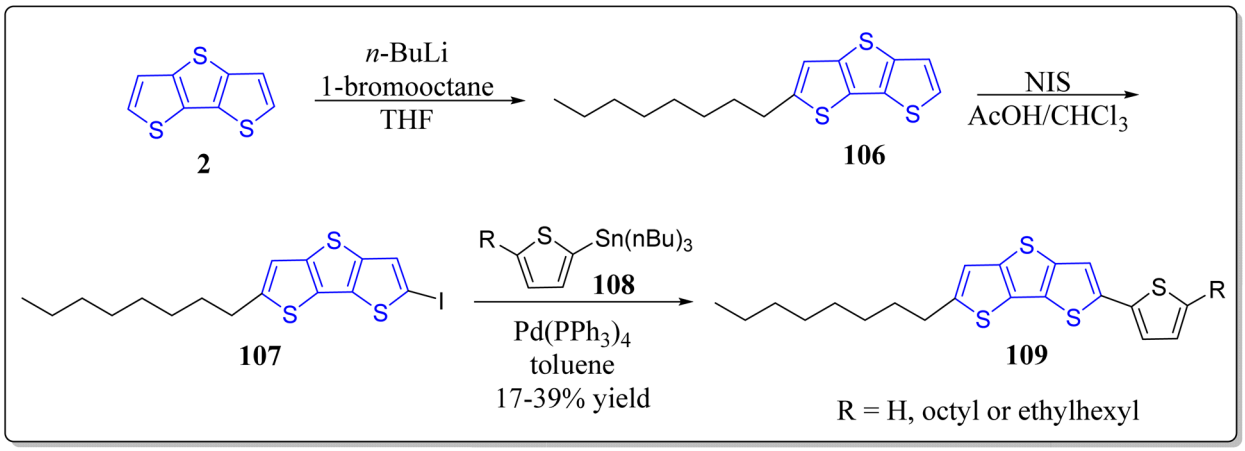

Scheme 16 Synthetic route for the preparation of asymmetric alkyl substituted DTT.

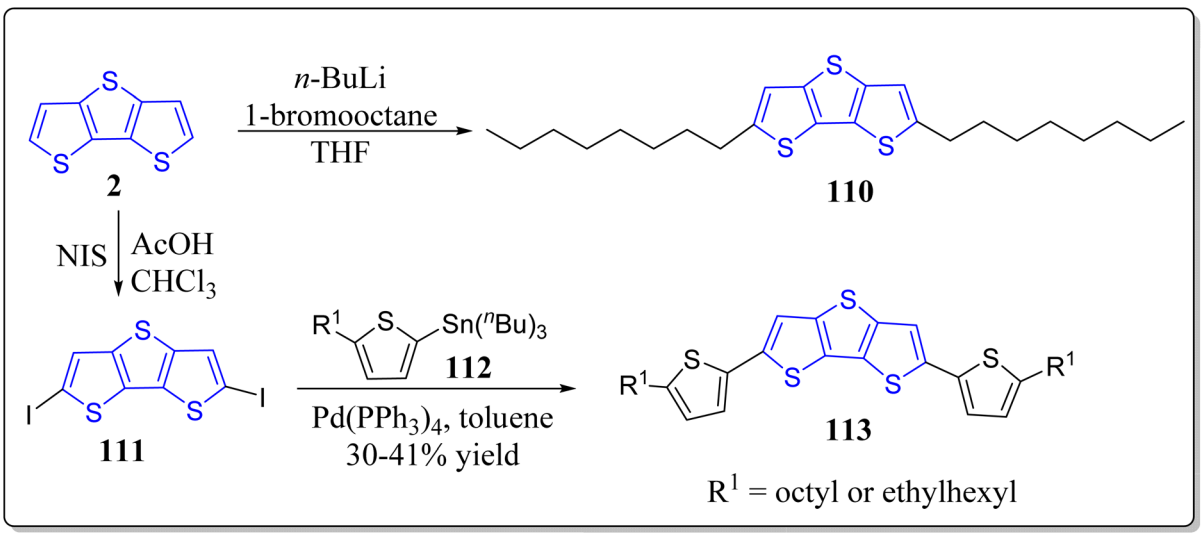

Scheme 17 Schematic generation of the symmetrically alkyl substituted DTT-based systems.

2.9. Applications of DTT-based expanded porphyrin architectures

In past few decades, designed and construction of the expanded porphyrins with large π-conjugation has gained a significant importance due to their diverse potential applications such as sensors, sensitizers for PDT, optoelectronic devices, NLO materials, models for the Hückel Möbius & Baird aromaticity *etc.* And fusion of one or more pyrroles in the extended porphyrins lead to the macrocyclic systems with rehabilitated electronic structures. Prompted from the immense potential of the core-modified expanded porphyrins,[102,103] Chandrashekar's research group has reported the fused porphyrins with DTT as a bridge (Scheme 18).[104] They reported 30π electrons heptaphyrin (**116**) and 34π electrons octaphyrin (**119**) *via* a feasible and effective synthetic strategy.[105] Both the systems were confirmed by means of spectroscopic as well as single crystal X-ray analysis, and showed the aromatic characteristics in protonated & free-base forms. Remarkably, on the first time protonation, in 34π doubly fused octaphyrins, one of the DTT ring experiences the ring flipping, however flipping of such large ring was not stated before in literature. Also, two types of hydrogen bonds were observed in 34π doubly fused octaphyrins *viz.* π···H–C (mesityl) and π···H–C (thiophene) which gives rise to self-assembled dimers. With this effective methodology, large expanded porphyrins can be easily accessed with the suitable precursors.

In a separate report, the same group has also reported a novel core reformed nonaphyrins **121** by the means of an operationally simple yet powerful methodology, displayed in the Scheme 19.[106] Interestingly, the X-ray and spectroscopic studies displayed a twisted Fig. 8 conformation in its nonaromatic as well as free-base arrangements. The protonation of pyrrole nitrogen provided a structural modification in which the Fig. 8 conformation changed into an open conformation having

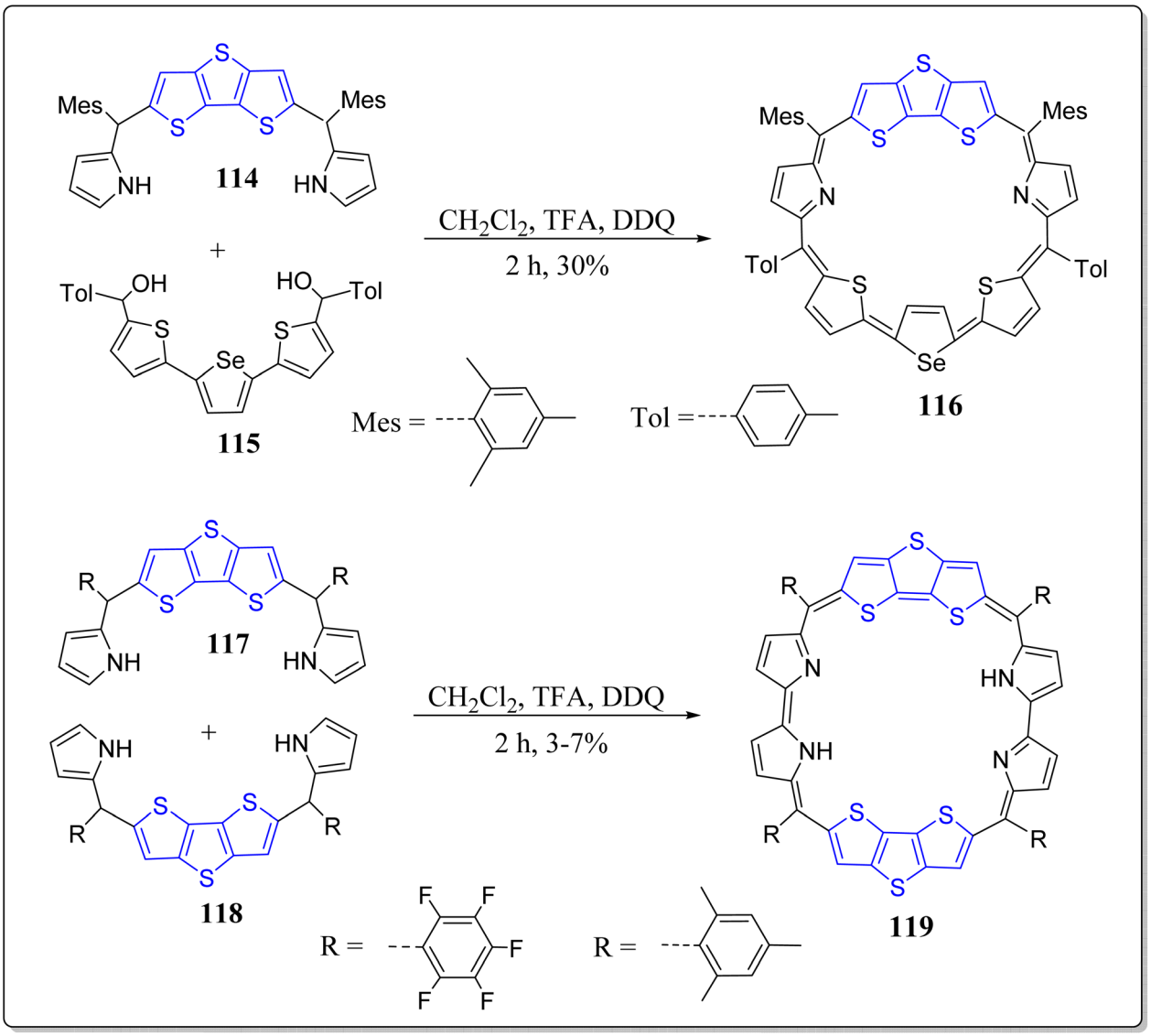

Scheme 18 Design and synthesis of heptaphyrin **116** & octaphyrin **119**.

inversion of pyrrole rings (Scheme 19). Notably, dications (**121**·2H$^+$) displayed $4n\pi$ Hückel antiaromatic character, reflected from spectral as well as theoretical studies. This versatile methodology gives great scope for the study of photophysical properties and coordination chemistry of non-fused and fused core modified nonaphyrins.

In the same context, Cha *et al.* has reported two virtuously organic non-planar DTT-bridged [34]octaphyrins **122** & **123**, accessing to two altered aromatic formulae as a function of the oxidation state having competing 26π & 34π-electronic circuits in their neutral forms (Scheme 19).[107] With two-electron oxidation, electronically mixed $[4n + 1]/[4n + 1]$ triplet biradical entities in the ground state were observed – displaying global aromaticity according to the Baird's rule. The excellency of this methodology can be displayed from the fact that it accessed two distinct dual aromatic molecules *via* a similar synthetic system and directs us to suggest that the conjugated bicyclic species play a significant role in widening the frontiers of aromaticity apart from the conceptual limits related to the Möbius and planar Hückel formulations. The authors have followed the same synthetic protocol as that of compound **124** and also compared the studies with the same system **124**. On the other hand, the research groups of Park & Kim has also studied the alterations in the macrocyclic aromaticity of the expanded porphyrin **122** by means of 1 : 1 C_{60} complex formation through π–π interactions in toluene.[108] From the nucleus independent chemical shift (NICS) calculations, absorption, emission & NMR spectroscopy means, the change in macrocyclic aromaticity was confirmed. Moreover, they exposed that the formation of the photoinduced charge-separated state & the triplet excited-state populations of the system can be controlled through a simple complexation with fullerene (C_{60}).

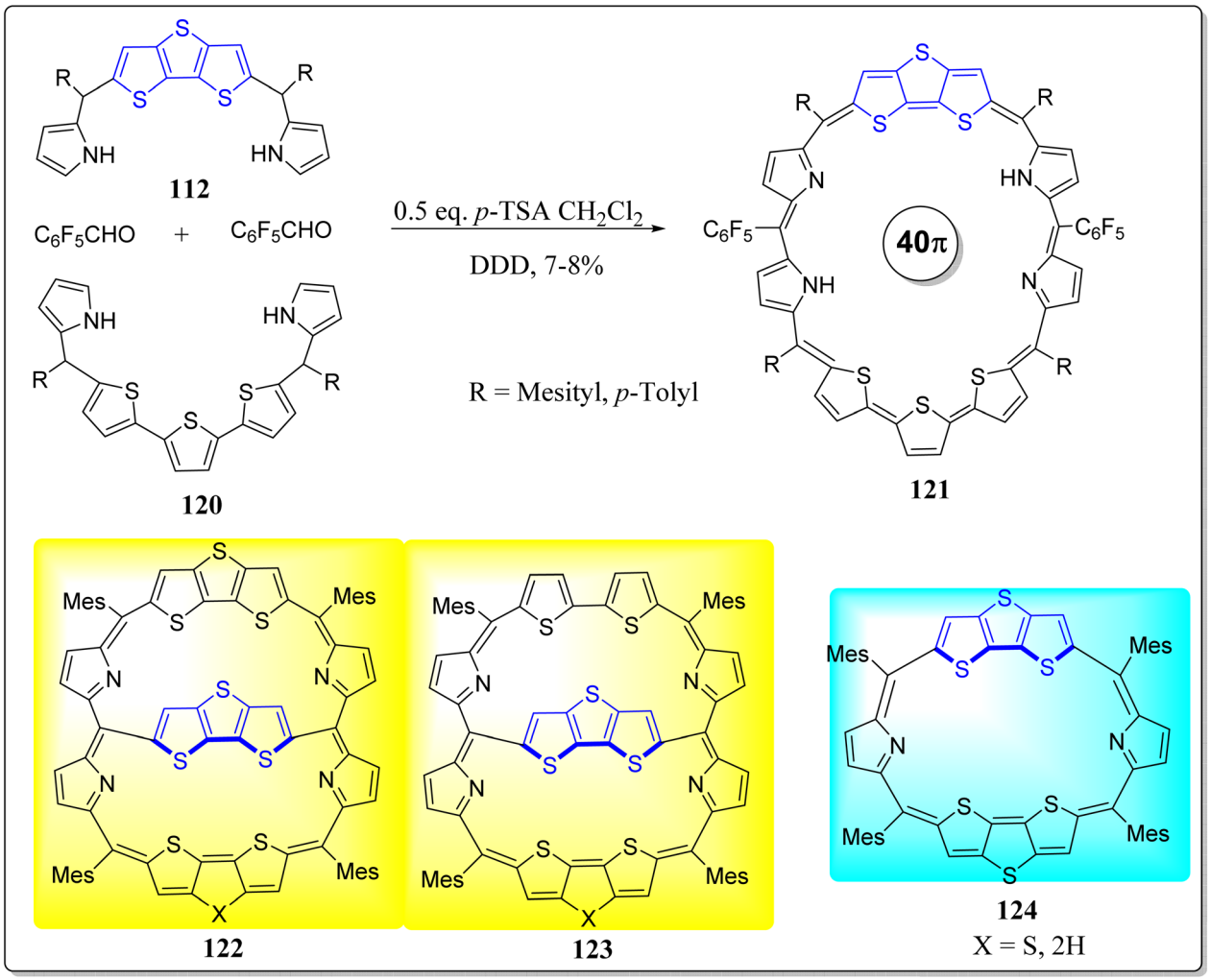

Scheme 19 Synthetic scheme for 40π conjugated core-modified nonaphyrins **121** and chemical structures of 3-D systems **122** & **123** along with reference compound **124**.

2.10. DTT-based mechanochemical chalcogen bonded cascaded switches

Recently, chalcogen-bonding cascade switching was presented to yield the vital chemistry tools desirable to image physical attractions in biological systems. Interestingly, fluorescence imaging of physical forces is one of the existing contests in biology which cannot go without any input from chemistry, thereby planarizable push–pull chromophores were led as a mechanosensitive fluorescent membrane probe.[109,110] To advance the flipper probes, Matile's research revealed operationally simple but cost effective DTT-based fluorescent mechanochemical chalcogen bonded cascade switches **125** & **126**, as shown in the Fig. 9.[111] In the classic flipper probe, a methyl group seemed to probably hinder the designed cascade switch. To avoid such inventions, elimination of the methyl group required the production of DTTs with distinct substitutions on the accessible carbons. Importantly, mechanosensitivity of the designed flipper probe was approximately similar to the original one. Hence, it can be stated that in flipper probes, the methyl groups in the switching section are insignificant to function, though they play a significant role in the twisting section. This delightful study endorses the concept of chalcogen bonded cascade switch and eradicates the synthetic technical hitches of single methyl elimination for future flipper probes broadenings.

In another report, the same group has effectively revealed the sulfoximines in the construction of fluorescent probes instead of sulfides, sulfones or sulfoxides (Fig. 10).[112] These vital flippers **127**, works as the mechanosensitive probe to image the tension as well as the order of the membrane. These authors trialed with the extra substitution of nitrogen atom, creating the differences in control and performances of the probes. In comparison to the traditional sulfone substituted flippers, the sulfoximine flippers absorption spectra were found to be red-shifted, besides the more intense emission maxima and extended fluorescence lifetime.

On the other hand, very recently, Afraj *et al.*, has demonstrated the heteroalkyl substitution effect on the 3,3′-

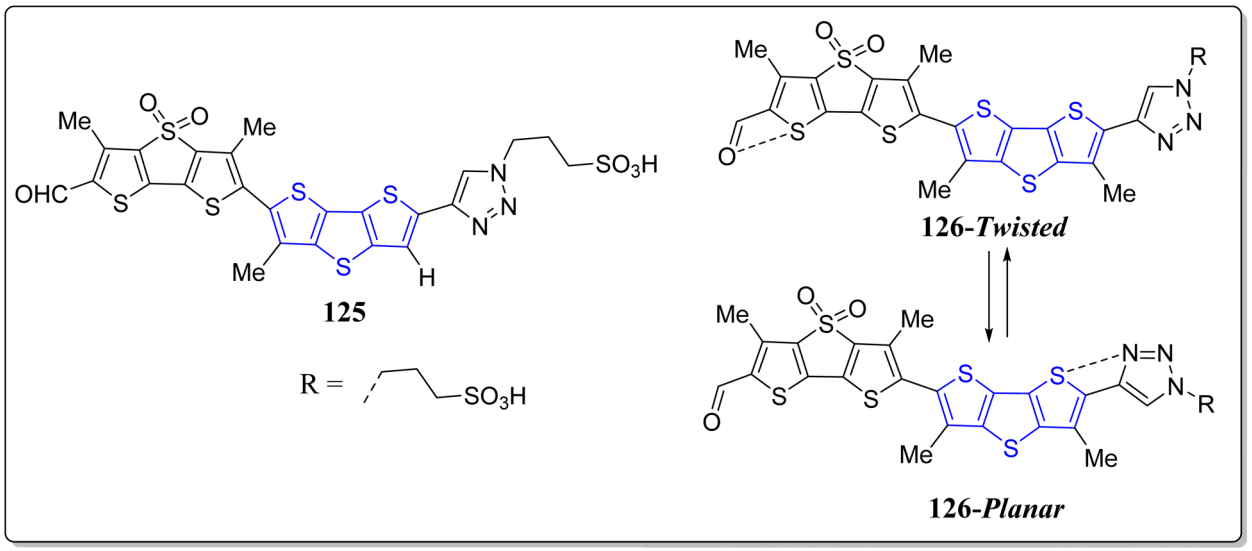

Fig. 9 Mechanochemical chalcogen-bonding cascade switches containing DTT.

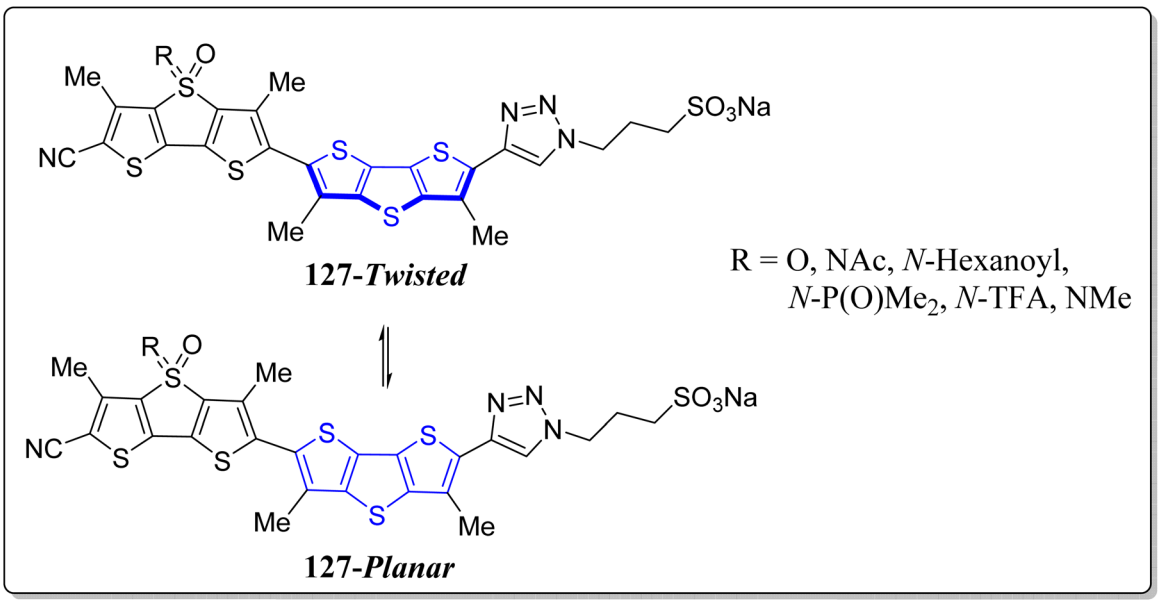

Fig. 10 Chemical structures of the twisted and planar forms of the sulfoximine flippers.

diheteroalkyl-2,2′-bithiophene based semiconductors.[113] They have successfully investigated the effects of the chalcogen series (O/S/Se), and also compared the characteristics of the chalcogen substituted compounds (**128–132**) (Fig. 11). Among the designed compounds, the highest carrier mobility was presented by the compound **128** (4.01 $cm^2 V^{-1} s^{-1}$), the maximum value reported till date for hole transporting materials in the case of fused thiophene based semiconductors. This incredible work done exhibited an extended viewpoint on the incorporation of chalcogen atom(s) in the π-conjugated core structures, and also showcased the relationship of the structure and properties for valuable organic semiconductors.

2.11. DTT as a versatile framework for dye sensitized solar cells (DSSCs)

Because of the renewable energy harvesting, numerous chief developments in the design of donor–π–acceptor (D–π–A) dyes have led to the eye-catching energy conversion efficiencies – novel materials are making it conceivable to generate the high power conversion and to produce an alternate power source for H_2 from H_2O under the sunlight. Remarkably, planning visible light active photocatalysts for solar energy conversion is being found to be one of the finest method to report the global energy glitches. In stark contrast, the DSSCs in the past couple of decades, have riveted the curiosity of the researchers globally

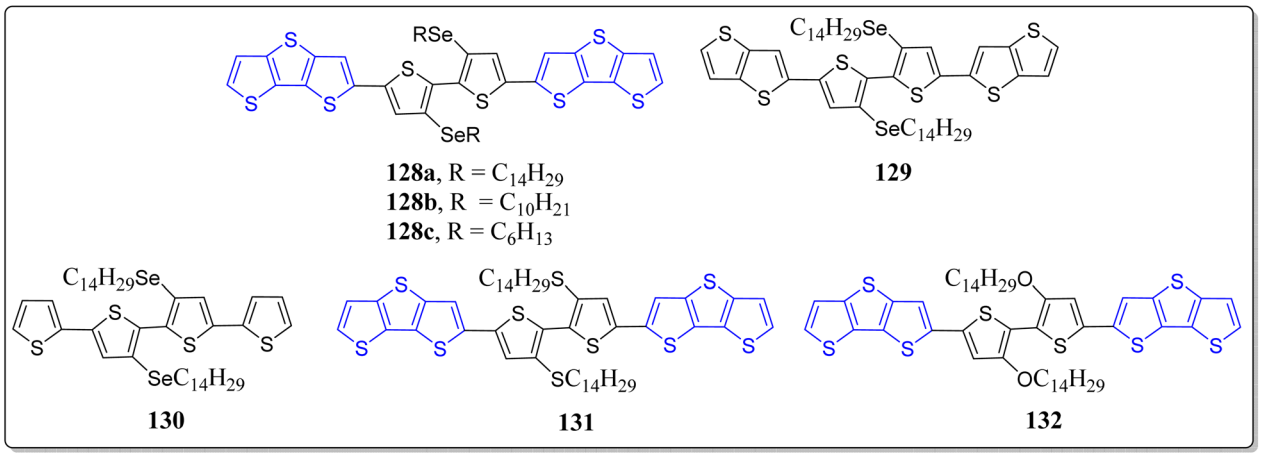

Fig. 11 The molecular structures of π-conjugated chalcogen-based semiconductors.

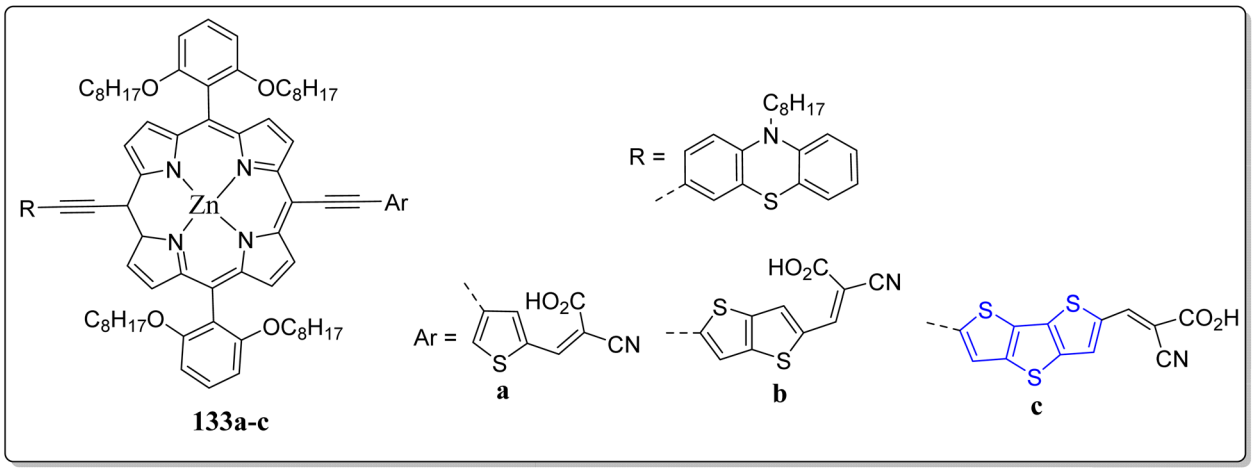

Fig. 12 Chemical structures of the porphyrin-based DSSC sensitizers **133a–c**.

because of their easy device construction, extraordinary PCE, and low cost *etc.* Particularly, the porphyrin based versatile sensitizers are highly efficient in the photocatalytic hydrogen production and DSSCs. In this regard, Gangadhar *et al.* revealed a photocatalytic hydrogen fabrication performance in the gradual order of 2691, 6641 & 7396 μmol g^{-1} h^{-1} by changing the thiophene (**133a**) to thienothiophene (**133b**) to DTT (**133c**) auxiliaries (Fig. 12).[114] Interestingly, by substituting the thiophene subunit in **133** with the thienothiophene & DTT, accomplished the remarkable PCE, 7.05% (**133b**) & 8.25% (**133c**) in DSSCs applications, and their high onset of Q-band absorption (720–750 nm), resulting in efficient harvesting of the sunlight. From the DFT calculations, they observed that the photoexcited intramolecular electron transfer (ET), from phenothiazine (donor) to cyanoacrylic (acceptor) took place through the porphyrin macrocyclic system. Finally, they concluded that this wonderful tactic of molecular engineering at the D & A fragments led to the competitive outcomes than to several literature reported sensitizers for both photocatalytic hydrogen generation as well as DSSC applications.

2.12. Applicability of DTT in aggregation-induced emission (AIE) active optical materials

Remarkably, geometrical organization of the organic functional materials in solid state, has an imperative control on their fluorescence as well as electroluminescence signatures. This crucial arrangement in the solid state, is dubbed as the aggregation-induced emission (AIE) which was established by the Tang *et al.*, and has attracted a great attention of the researchers worldwide in the several past years. In this line, tetraphenylethylene (TPE) – possessing excellent AIE property, is known as a non-emissive chromophore in solution & highly emissive in solid state because of its twisted structure. On the other front, thieno[3,2-*b*]thiophenes (TT), is a rigid electron-rich framework with an extended π-conjugation, making them appropriate for fine-tuning the band-gap (low) of organic functional materials and increasing the intermolecular interactions in the solid state to produce the conjugated low band-gap organic semiconductors. Importantly, fusing another thiophene moiety to TT, deliver the DTT, which is widely used to form gifted organic materials due to their electron richness,

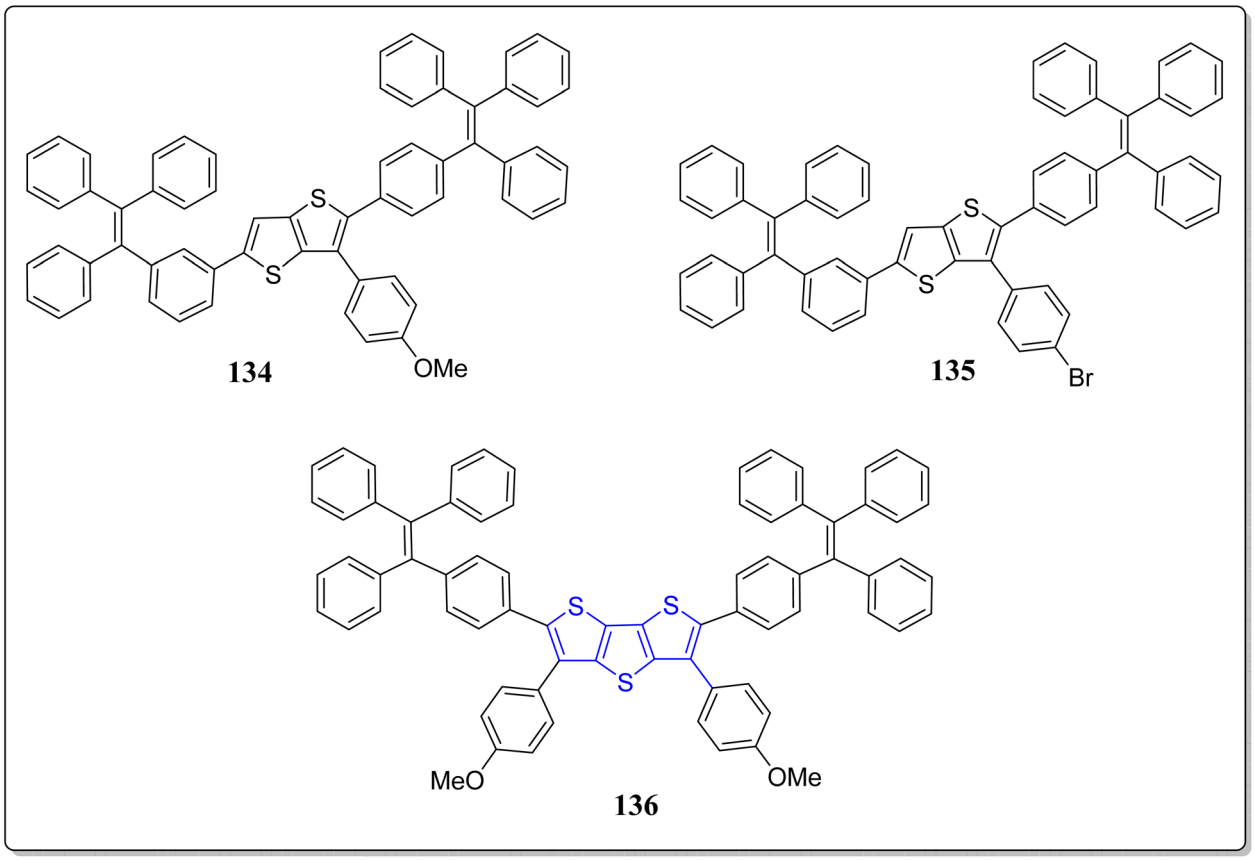

Fig. 13 The structures of TPE substituted TT & DTT derivatives (**134–136**) for OLEDs.

rigid, & flat delocalized systems. As organic materials made of TTs & DTTs demonstrate interesting features in conducting as well as semiconducting devices, for instance OLEDs, OSCs and OFETs. Therefore, a handful of such materials have been reported in the literature for diverse applications.[115] In this context, the research team of Ozturk revealed the peripherals TPE substituted TT & DTT derivatives (**134–136**) for AIE applications at OLEDs, as shown in the Fig. 13.[116] The properties of these handy systems were probed by means of computational & experimental studies besides the X-ray diffraction & DFT-optimization. Different substitution positions of the TPE on substrates, generated the dramatic result on AIE as well as optical properties. The TT-based systems produced an outstanding device performance – maximum luminance = 11 620 cd m^{-2}, maximum external quantum efficiency = 2.43%, and a maximum current efficiency = 6.17 cd A^{-1}. The synthesized architectures showed temperature tolerance up to 500 °C, and this thermal stability is vastly suitable for the fabrication of OLED devices, and this work may provide an excellent strategy to further develop the DTT-based electroluminescence resources in the later generations.

2.13. DTT-based thienoacenes

Vegiraju *et al.* has demonstrated a simpler yet efficient synthetic protocol to construct the solution processable small molecular semiconductors (**143**) possessing thiophene, TT & DTT in its core structure, prepared *via* a one-pot [1 + 1 + 1] strategy, for OFETs applications (Scheme 20).[117] These authors investigated the computed electronic framework, electrochemical and optical properties of thus prepared molecules, and also contrasted with the non-thiolated 3,5-dialkyl dithienothiophene based systems. Notably, the single crystal analysis endorsed the idea of S···S intramolecular lock structure (S···S) through one sulfur atom of the alkyl group and another sulfur of thiophene with a short distance of 3.17 Å. This framework not just only exhibited the structure equivalent to *n*-thienoacenes but also supports planarity and extensive π-conjugation. The significance of this tactic can be inspected from the high value of OFET hole mobility (2.6 cm^2 V^{-1} s^{-1}) in comparison to other reported *n*-thienoacenes. Moreover, in a separate work, the same research group has also reported p-type organic semiconductors for OFETs applications, based on the core alkyl substituted tetrathienoacene (TTAR) **144–146** consisting of T, TT & DTT as the end capped moieties (Fig. 14).[118] Among the synthesized organic semiconductors **144–146** from the building block **147**, the one end capped with the DTT (**146**), presented the best results for OFETs – resulting high hole mobility (0.81 cm^2 V^{-1} s^{-1}) as well as the molecular interactions in film form. These workers also commented that it was the highest mobility found at that time for a solution-processable p-type TTAR-based molecular semiconductors.

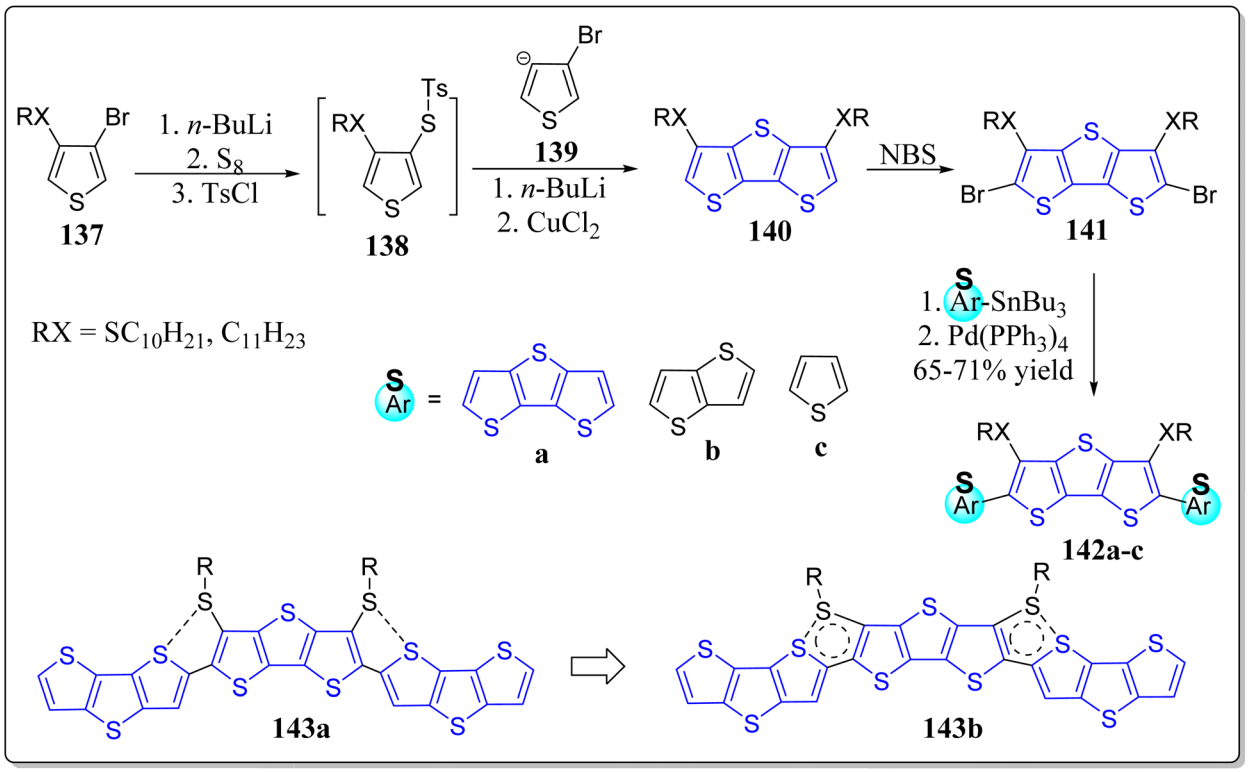

Scheme 20 Solution processable pseudo *n*-thienoacenes through intramolecular S···S lock.

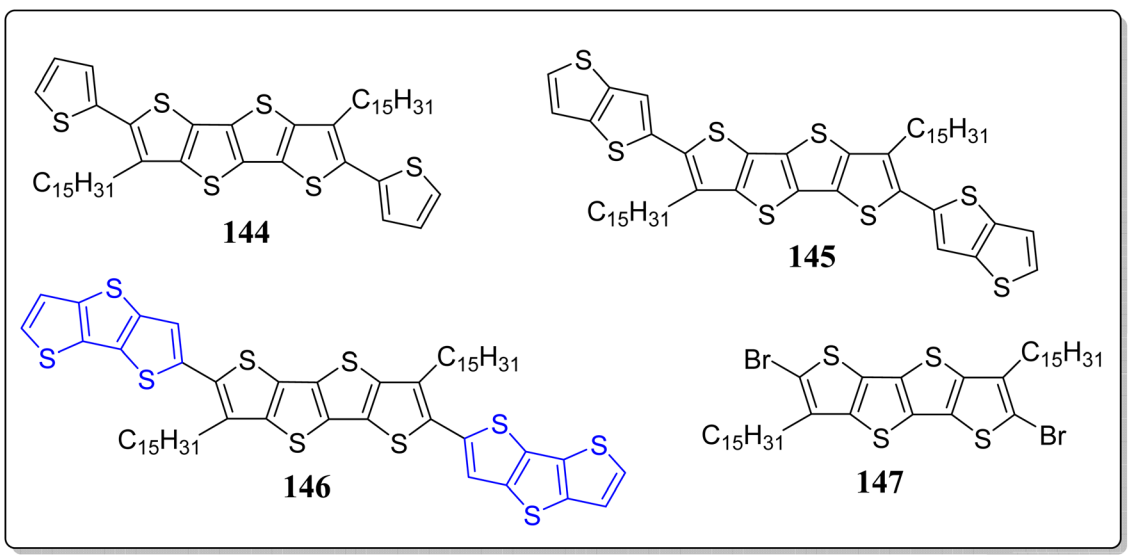

Fig. 14 Construction of TTAR based semiconductors having T, TT & DTT end groups.

On the other hand, for the application of OFETs, the DTT-based small molecular semiconductor **153** and 1-insulating polymer blends **154** were described by Lin *et al.* (Scheme 21).[119] Electrochemical, thermal, and optical features of these systems were extensively examined, and compared with the other similar type architectures. From the single crystal analysis of **155**, they observed intramolecular lock between S(thiophene)··· S(alkyl), at a distance of 3.10 Å with a planar core structure. Remarkably, the system **153** in an OFET device, showed the hole mobility of 3.19 $cm^2\ V^{-1}\ s^{-1}$ in environmentally friendlier solvent, namely anisole by means of solution-shearing deposition technique – the highest reported value for an all-thiophene based small molecular semiconductor at that time. The reason for this high value were attributed because of coplanarity of the core structure, co-facial π–π stacking and extended π-conjugation. Moreover, insulating polymer **154** devices and blend

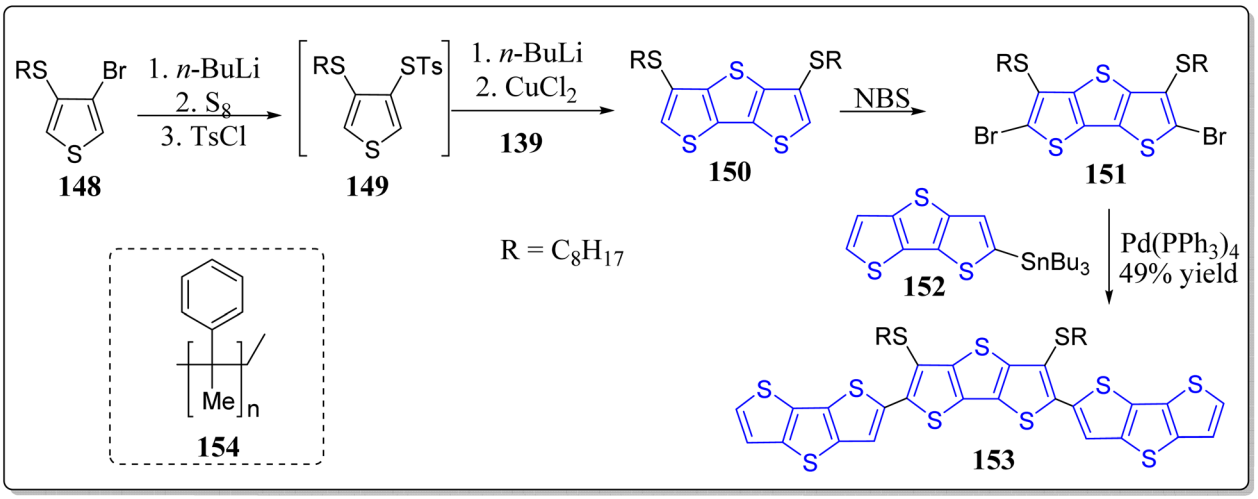

Scheme 21 Synthesis of **153** and the chemical structures of 1-insulating polymer blend **154**.

films were also inspected. The morphological analysis divulges a nanoscopic vertical phase separation with the **154** layer preferentially communicating the dielectric & **153** positioned on top of stack and the manifestation of greatly textured and connected semiconductor phases for as little as 10% of the semiconductor content. The OFET based on the blend containing 50% weight of **153** showed a hole mobility of 2.44 $cm^2 V^{-1} s^{-1}$ & a smaller threshold voltage shift under the gate bias stress. In comparison to devices with pristine semiconductor film, these devices displayed greater bias stress stability and storage capacity. This advanced approach contributes to the solution processed molecule-insulating polymer blends under eco-friendly solvent, and also established the correlation between the electronic response of the stratified corresponding OFETs and crystalline structure.

In recent years, heteroacenes containing fused five membered aromatic ring moieties like thienoacenes and *S*,*N*-heteroacenes has drawn a sizeable attention of the scientific community, as they were found the key building blocks for the generation of high-performance organic electronic smart materials and devices. Amongst, a variety of heteroatoms selenium (Se) has only scarcely been employed into the aromatic rings, may be due expensiveness of selenophene itself, and also because of an inadequate number of commercial availability of its derivatives, hence its chemistry is less explored and needed to be exploited to the advanced level. To this context, selenophene-containing heterotriacenes through the C–Se coupling and/or copper-catalyzed cyclization as key steps in multistep synthetic approach has fruitfully been reported by the Schwartz *et al.* (Scheme 22)[120] In this paper, the authors have not only prepared the DTT system **2** by an alternative route but also assembled its Se-substituted tricyclic congeners **155–157**. The single X-ray crystal structure and XRD powder analysis were employed for their chemical structures determination & packing motifs establishment. Furthermore, the quantum chemical calculations provided the deeper knowledge of the electronic & geometric structures of these systems. These heterotriacenes were found to be very stable and nicely soluble in the organic solvents, thereby their electrochemical, optical, and thermal properties were determined with ease. From the comparison of optoelectronic studies, structure–property relationships (SARs) provided the valuable understandings of the

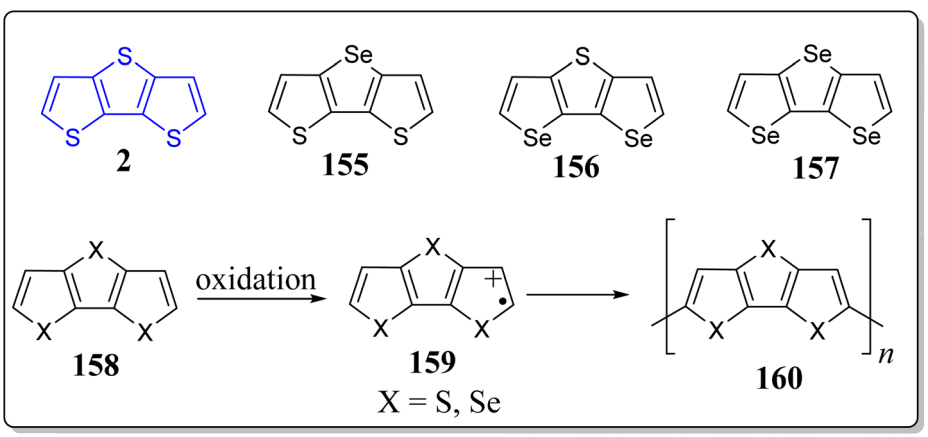

Scheme 22 Structures of S/Se-substituted heterocycles & oxidative polymerization of them.

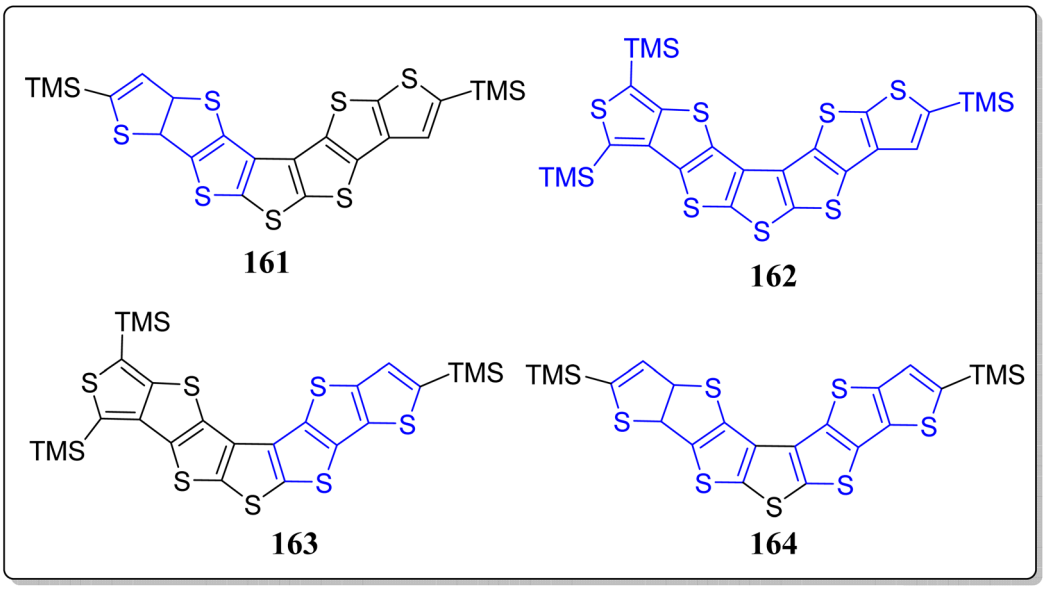

Fig. 15 Structures of heptathienoacenes and (un)symmetrical heptathienoacenes.

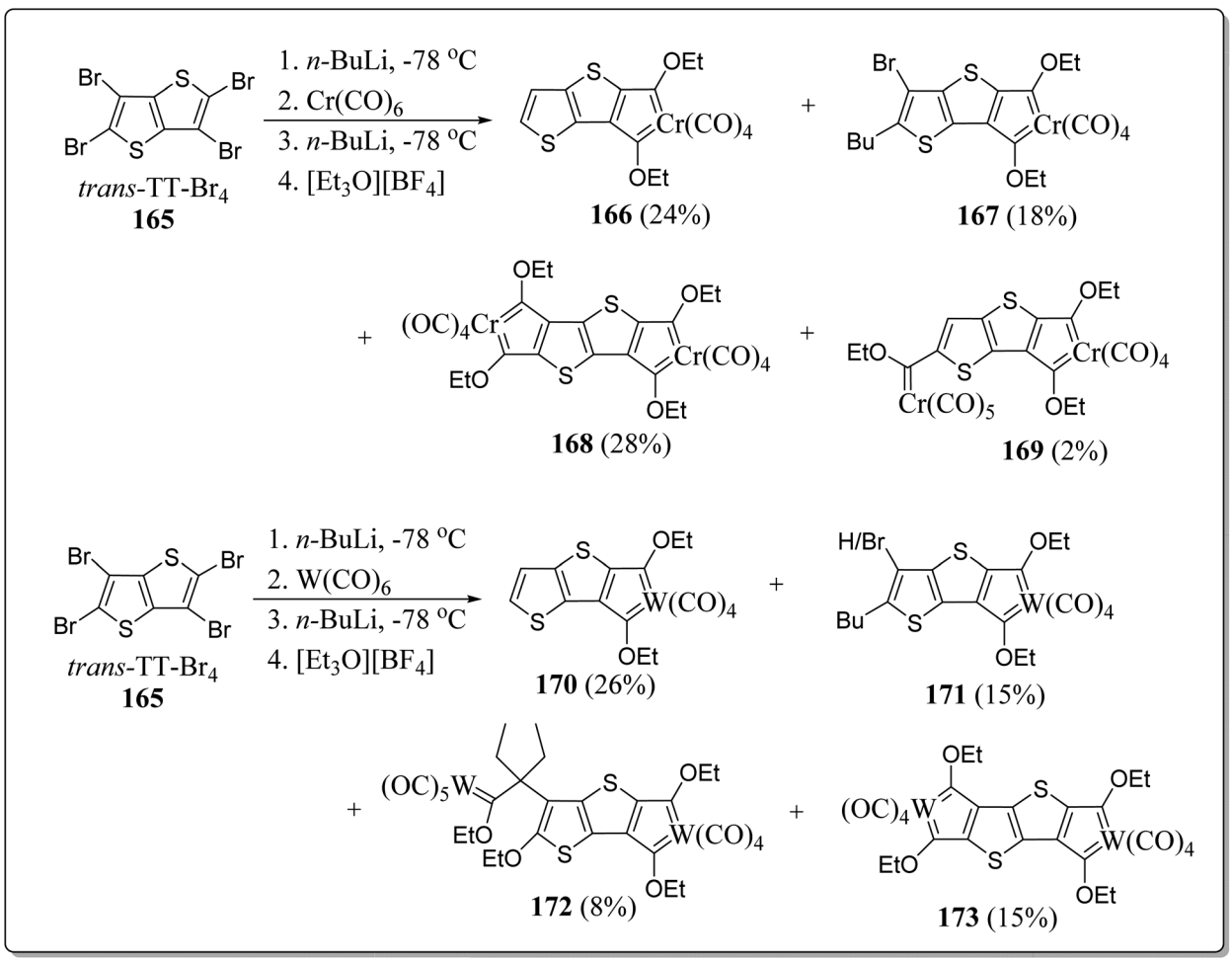

Scheme 23 Construction of chelated Fischer carbene complexes.

role of heteroatoms in thus synthesized heterotriacenes. Lastly, the electrooxidative polymerization of the triacenes **2** & **155–157** afforded the corresponding polymeric materials **160** (Scheme 22). These conducting polymers were characterized through spectrochemically as well as electrochemically, and their properties were also compared to that of non-bridged counterparts.

Basically, balancing as well as controlling the isomeric position of sulfur atoms in the thienoacenes is crucial tactic to tune the signatures of the intermolecular interactions and intramolecular π-conjugation. In this regard, Wang's research group has reported three unsymmetrical (**161–163**) and one symmetrical (**164**) bull's horn-shaped heptathienoacenes whose chemical structures are depicted in the Fig. 15.[121] Synthesis of these versatile systems were accomplished by means of the Suzuki–Miyaura cross-coupling reaction and intramolecular cyclization as key steps. Owing to the presence of intermolecular interactions and/or molecular π-electronic conjugations, both in solution and crystalline forms, the studies of crystal analysis, UV-vis absorption spectroscopy, electrostatic potential measurement, CV and fluorimetry displayed the notable SARs. The suitable location of sulfur atoms in thienoacenes encourages a new methodology for the construction of high-level thienoacenes through mutable molecular frameworks created by the Pd-catalyzed cross-coupling of the distinct low-level thienoacene moieties (DTT). With the development of novel molecular networks, thienoacenes will showcase vital applications in organic photovoltaics, & OFET, *etc.*

2.14. Role of DTT-skeleton in chelated carbene complexes

The oligothiophene and its congeners are tempting units which acts as the spacer-ligand(s) between metal fragments for impending long distance metal–metal communication. On the other front, electron rich thiophene donors and strong electron-poor 'Fischer carbene' carbon acceptors showcased in a 'push–pull' manner through a conjugated path is conducive to electron transfer and polarization practices with a variety of electronic applications. Bearing the these points in mind, Lamprecht *et al.* produced semi-circular and linear chelated mononuclear bis-carbene as well as binuclear tetracarbenes having *trans*-DTT/TT, and *cis*-DTT/TT insertions (Schemes 23 & 24).[122] The synthesized molecules displayed an overall linear molecular geometry on engaging *trans*-DTT or TT insertions *e.g.* **168**, **173**, **176** & **182**, and also the semicircular/bent molecular geometry were observed with the complexes with *cis*-DTT insertions. By means of DFT calculations, and the redox events, electronic delocalization and the possibility of intramolecular metal–metal communication were examined. Moreover, the electronic properties of these systems were also investigated by CV experimentations and were contrasted with non-chelated Fischer-type monocarbene compounds. The experimentation specified that the reduction of chelated carbene compounds resulted in delocalization of negative charge all over the carbene carbon atoms. However, the reduction of chelated carbene compounds is more effortless in comparison to monodentate carbene compounds. Further, the dissimilarities of electronic

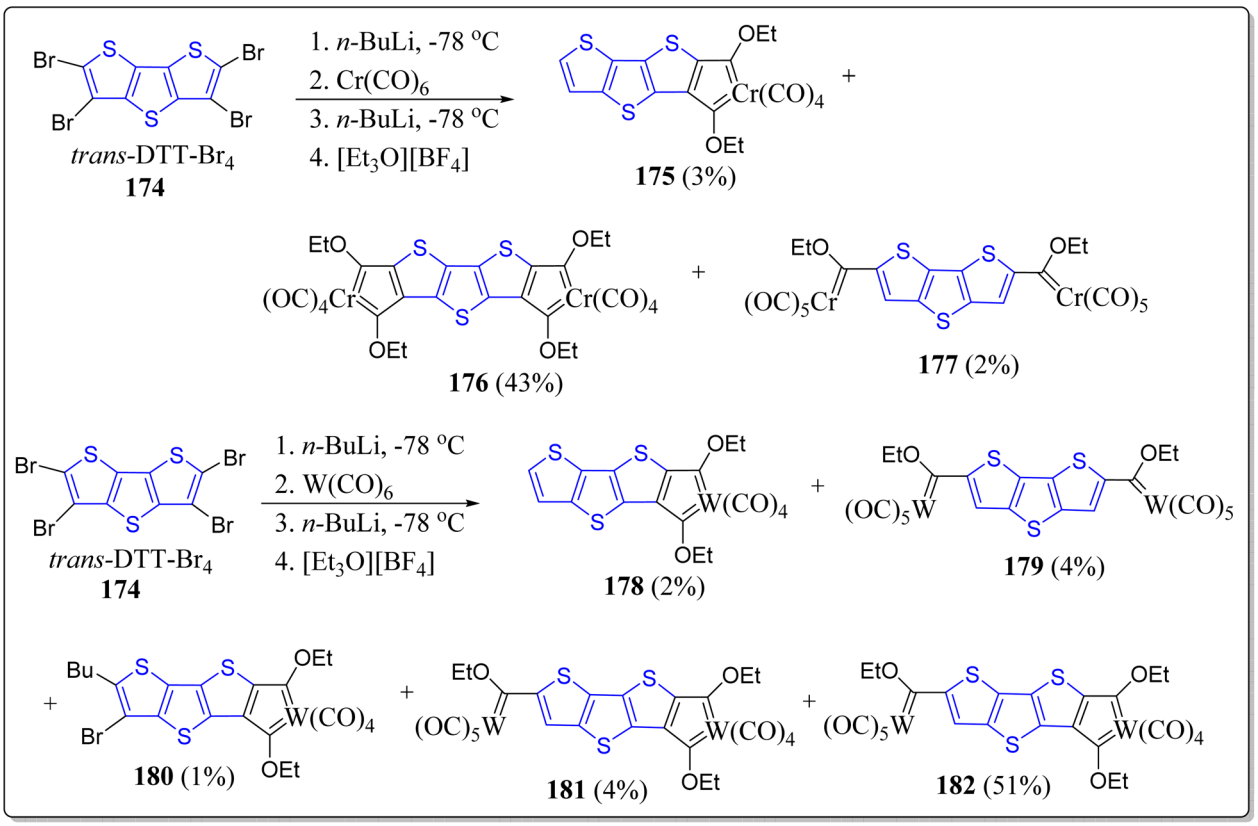

Scheme 24 Designed synthesis of the chelated carbene complexes.

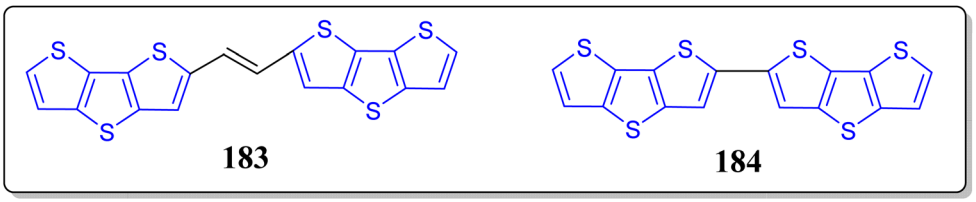

Fig. 16 Chemical structures of organic radical semiconductors **183** & **184**.

properties of these conjugated chelated compounds were compared with the chelated carbene compounds without taking into account the linear conjugated pathway. In the event of chelated carbene compounds, with linear conjugated insertions, the delocalization of negative charge is all across the thienylene carbons and adjacent sulfur atoms. Such delocalization of sulfur electrons imparts in the LUMO of the compounds and results in reduction at the lesser negative site in comparison to bent non-conjugated with *cis*-DTT insertions, where the contribution from sulfur atoms are absent and generate the radical anions and do not approve a planar arrangement by a co-planar carbene carbon.

2.15. Applications of DTT-based systems in radical semiconductors

The organic electronics is recognized as the next generation of electronics, proposing benefits like solution processability, flexibility, and low costs *etc.* And the organic semiconductors are vital constituents of the organic electronic which are fairly different from their inorganic counterparts due to their structural diversities – and allowing to adjust the material properties by virtue of molecular engineering. On the other hand, organic radicals are comprehensively explored in the field of magnetic materials and OFETs, but the devices with organic radical semiconductors are uncommon because of the instability of these types of molecules.[123,124] To produce an efficient strategy for the stable radical(s) with excellent magnetic as well as electrical properties, Zhang *et al.* reported two almost similar molecular structure based organic radical semiconductors **183** and **184** (Fig. 16).[125] It has been noticed by the authors that **183** behaves in the manner of standard p-type organic semiconductor, whereas **184** demonstrates great conductivity, as a result of an enormous upsurge in the hole density because of the generation of radicals. Furthermore, they observed that **184** is more stable and the charge density can be reversibly monitored by means of thermal de-doping. These outcomes exhibit electrical behaviors of the systems, which can be adjusted easily through the charge transfer complex radicals, and can open-up new ideas for the construction of emerging devices promoted by stimulating mediators.

3. Summary and outlook

Owing to the remarkable properties of the conjugated heterocyclic materials, they have become appealing players in various fields, and growing day-by-day. Among them thiophene-based architectures in general and DTT-based systems in particular have revolutionized the area of organic electronics. Herewith, synthetic strategies, properties, and the interesting applications of the DTT-based systems in the formation of electronic devices has been revealed in detailed. In this particular review article, we have exposed diverse uses of DTT-based molecules *viz.* organic photodetectors, dye sensitized solar cells, AIE active optic materials, planarizable push–pull probes, *etc.* A wide range of DTT-based moieties with different substitutions, like, alkyl chains, aromatic rings, electron-withdrawing groups, halogens and their contribution in diverse applications have been discussed. This article highlights the importance of π-conjugated system in the performance of electronic devices, particularly DTT, who's excellent π-conjugation, reduced band gap, high charge carrier mobility, *etc.* makes it an electron rich vital building block. In the present review article, we have tried to highlight the versatility, applicability, and the advancements made in the DTT-based arena from 2015 to till date. Hopefully, this updated write-up on the DTT scaffold will be very useful to the readers, and will provide ideas for future work.

Conflicts of interest

There are no conflicts to declare.

Acknowledgements

We are appreciative to the DST-SERB New Delhi for financial support (Project File no. ECR/2017/000821), and also grateful to Jamia Millia Islamia, New Delhi for research facilities.

References

1 (*a*) Z. Xue, S. Chen, N. Gao, Y. Xue, B. Lu, O. A. Watson, L. Zang and J. Xu, *Polym. Rev.*, 2020, **60**, 318–358; (*b*) S. Alvi and R. Ali, *Beilstein J. Org. Chem.*, 2020, **16**, 2212–2259; (*c*) S. Alvi and R. Ali, *Beilstein J. Org. Chem.*, 2021, **17**, 1374–1384; (*d*) R. Ali and S. Alvi, *Tetrahedron*, 2020, **76**, 131345; (*e*) S. A. Wagay, I. A. Rather and R. Ali, *ChemistrySelect*, 2019, **4**, 12272; (*f*) M. Saito, H. Shinokubo and H. Sakurai, *Mater. Chem. Front.*, 2018, **2**, 635–661.

2 (*a*) R. Fringuelli, L. Milanese and F. Schiaffella, *Mini-Rev. Med. Chem.*, 2005, **5**, 1061; (*b*) W. Ahmed, V. Jayant, S. Alvi, N. Ahmed, A. Ahmed and R. Ali, *Asian J. Org. Chem.*, 2022, **11**, e202100753; (*c*) P. K. Gupta, M. K. Hussain, M. Asad, R. Kant, R. Mahar, S. K. Shuklac and K. Hajela, *New J. Chem.*, 2014, **38**, 3062–3070.

3 I. A. Rather and R. Ali, *ACS Omega*, 2022, **7**, 10649–10659.
4 S. Kotha and R. Ali, *Tetrahedron Lett.*, 2015, **56**, 2172–2175.
5 S. Kotha and R. Ali, *Synthesis*, 2014, **46**, 2471–2480.
6 S. Kotha, R. Ali and A. Tiwari, *Synlett*, 2013, **24**, 1921–1926.
7 S. Kotha, R. Ali and A. K. Chinnam, *Tetrahedron Lett.*, 2014, **55**, 4492–4495.
8 S. Kotha and R. Ali, *Tetrahedron Lett.*, 2015, **56**, 3992–3995.
9 I. A. Rather and R. Ali, *ChemistrySelect*, 2021, **6**, 10948–10956.
10 M. I. Ansari, R. Shankar, M. K. Hussain, R. Kant, P. R. Maulik, K. R. Kumar and K. Hajela, *J. Heterocycl. Chem.*, 2011, **48**, 1336–1341.
11 S. Alvi and R. Ali, *Org. Biomol. Chem.*, 2021, **19**, 9732–9745.
12 R. Ali and R. Siddiqui, *Adv. Synth. Catal.*, 2021, **363**, 1290–1316.
13 R. Siddiqui and R. Ali, *Beilstein J. Org. Chem.*, 2020, **16**, 248–280.
14 S. Kotha and R. Ali, *J. Chem. Sci.*, 2019, **131**, 66.
15 J. Pak, R. Ali and J. S. Park, *Bull. Korean Chem. Soc.*, 2016, **37**, 732–735.
16 S. Kotha and R. Ali, *Tetrahedron*, 2015, **71**, 6944–6955.
17 K. Strakova, L. Assies, A. Goujon, F. Piazzolla, H. V. Humeniuk and S. Matile, *Chem. Rev.*, 2019, **119**, 10977–11005.
18 F. Dikcal, T. Ozturk and M. E. Cinar, *Org. Commun.*, 2017, **10**, 56–71.
19 W. Wu, Y. Liu and D. Zhu, *Chem. Soc. Rev.*, 2010, **39**, 1489–1502.
20 L. Chen, M. Baumgarten, X. Guo, M. Li, T. Marszalek, F. D. Alsewailem, W. Pisula and K. Müllen, *J. Mater. Chem. C*, 2014, **2**, 3625–3630.
21 H. Wang, W. Xu and D. Zhu, *Dyes Pigm.*, 2013, **97**, 303–310.
22 L. San Miguel, W. W. Porter and A. J. Matzger, *Org. Lett.*, 2007, **9**, 1005–1008.
23 W. Hong, H. Yuan, H. Li, X. Yang, X. Gao and D. Zhu, *Org. Lett.*, 2011, **13**, 1410–1413.
24 J. Frey, A. D. Bond and A. B. Holmes, *Chem. Commun.*, 2002, 2424–2425.
25 P. Oechsle and J. Paradies, *Org. Lett.*, 2014, **16**, 4086–4089.
26 T. Bruton, *Sol. Energy Mater. Sol. Cells*, 2002, **72**, 3–10.
27 M. Wang, Q. Fan and X. Jiang, *Org. Lett.*, 2016, **18**, 5756–5759.
28 A. Mishra and P. Bäuerle, *Angew. Chem., Int. Ed.*, 2012, **51**, 2020–2067.
29 K. Olech, R. Gutkowski, V. Kuznetsov, S. Roszak, J. Sołoducho and W. Schuhmann, *ChemPlusChem*, 2015, **80**, 679–687.
30 M. E. Cinar and T. Ozturk, *Chem. Rev.*, 2015, **115**, 3036–3140.
31 I. A. Rather, F. A. Sofi, M. A. Bhat and R. Ali, *ACS Omega*, 2022, **7**, 15082–15089.
32 S. A. Wagay, I. A. Rather and R. Ali, *Mater. Today: Proc.*, 2021, **36**, 657–678.
33 I. A. Rather, S. A. Wagay and R. Ali, *Coord. Chem. Rev.*, 2020, **415**, 213327.
34 (*a*) I. A. Rather, S. A. Wagay, M. S. Hasnain and R. Ali, *RSC Adv.*, 2019, **9**, 38309–38344; (*b*) J. Y. Lee, H. D. Root, R. Ali, W. An, V. Lynch, S. Bähring, I. S. Kim, J. L. Sessler and J. S. Park, *J. Am. Chem. Soc.*, 2020, **142**(46), 19579–19587; (*c*) A. Kim, R. Ali, S. H. Park, Y. H. Kim and J. S. Park, *Chem. Commun.*, 2016, **52**, 11139–11142.
35 I. A. Rather and R. Ali, *Org. Biomol. Chem.*, 2021, **19**, 5926–5981.
36 I. F. Perepichka, D. F. Perepichka, H. Meng and F. Wudl, *Adv. Mater.*, 2005, **17**, 2281–2305.
37 G. Barbarella, M. Melucci and G. Sotgiu, *Adv. Mater.*, 2005, **17**, 1581–1593.
38 A. Capan, H. Veisi, A. C. Goren and T. Ozturk, *Macromolecules*, 2012, **45**, 8228–8236.
39 J. Roncali, P. Blanchard and P. Frère, *J. Mater. Chem.*, 2005, **15**, 1589–1610.
40 (*a*) T.-H. Kwon, V. Armel, A. Nattestad, D. R. MacFarlane, U. Bach, S. J. Lind, K. C. Gordon, W. Tang, D. J. Jones and A. B. Holmes, *J. Org. Chem.*, 2011, **76**, 4088–4093; (*b*) F. Osterod, L. Peters, A. Kraft, T. Sano, J. Morrison, N. Feederc and A. B. Holmes, *J. Mater. Chem.*, 2001, **11**, 1625–1633; (*c*) X. C. Li, H. Sirringhaus, F. Garnier, A. B. Holmes, S. C. Moratti, N. Feeder, W. Clegg, S. J. Teat and R. H. Friend, *J. Am. Chem. Soc.*, 1998, **120**, 2206–2207; (*d*) J. Frey, A. D. Bond and A. B. Holmes, *Chem. Commun.*, 2002, 2424–2425.
41 (*a*) H. Qin, S. Wenger, M. Xu, F. Gao, X. Jing, P. Wang, S. M. Zakeeruddin and M. Grätzel, *J. Am. Chem. Soc.*, 2008, **130**, 9202–9203; (*b*) S. Zhang, Y. Guo, H. Xi, C. Di, J. Yu, K. Zheng, R. Liu, X. Zhan and Y. Liu, *Thin Solid Films*, 2009, **517**, 2968–2973.
42 A. B. Marco, R. Andreu, S. Franco, J. Garín, J. Orduna, B. Villacampa and R. Alicante, *Tetrahedron*, 2013, **69**, 3919–3926.
43 H. Muraoka, Y. Watanabe, A. Takahashi, H. Kamoto and S. Ogawa, *Heteroat. Chem.*, 2014, **25**, 473–481.
44 M. Shellaiah, H.-P. Fang, Y.-L. Lin, Y.-C. Hsu, J.-T. Lin and H.-C. Lin, *Tetrahedron*, 2013, **69**, 2124–2130.
45 T. I. Ryu, Y. Yoon, J.-H. Kim, D.-H. Hwang, M. J. Ko, D.-K. Lee, J. Y. Kim, H. Kim, N.-G. Park, B. Kim and H. J. Son, *Macromolecules*, 2014, **47**, 6270–6280.
46 C.-Y. Lee, B. Kim, K. H. Kim, Y. Yoon, M. W. Lee, D. H. Choi, M. J. Ko, H. Kim, D.-K. Lee and K. Kim, *Synth. Met.*, 2013, **164**, 64–68.
47 W. Ni, M. Li, B. Kan, Y. Zuo, Q. Zhang, G. Long, H. Feng, X. Wan and Y. Chen, *Org. Electron.*, 2014, **15**, 2285–2294.
48 S. J. Lou, J. M. Szarko, T. Xu, L. Yu, T. J. Marks and L. X. Chen, *J. Am. Chem. Soc.*, 2011, **133**, 20661–20663.
49 T. Abidin, Q. Zhang, K.-L. Wang and D.-J. Liaw, *Polymer*, 2014, **55**, 5293–5304.
50 V. K. Thakur, G. Ding, J. Ma, P. S. Lee and X. Lu, *Adv. Mater.*, 2012, **24**, 4071–4096.
51 Y.-J. Cheng, S.-H. Yang and C.-S. Hsu, *Chem. Rev.*, 2009, **109**, 5868–5923.
52 K. T. Kamtekar, A. P. Monkman and M. R. Bryce, *Adv. Mater.*, 2010, **22**, 572–582.
53 C. Wang, H. Dong, W. Hu, Y. Liu and D. Zhu, *Chem. Rev.*, 2012, **112**, 2208–2267.

54 W. T. Neo, Q. Ye, T. T. Lin, S. J. Chua and J. Xu, *Sol. Energy Mater. Sol. Cells*, 2015, **136**, 92–99.
55 A. Kumar, D. M. Welsh, M. C. Morvant, F. Piroux, K. A. Abboud and J. R. Reynolds, *Chem. Mater.*, 1998, **10**, 896–902.
56 C. Ma, M. Taya and C. Xu, *Polym. Eng. Sci.*, 2008, **48**, 2224–2228.
57 Q. Ye, W. T. Neo, C. M. Cho, S. W. Yang, T. Lin, H. Zhou, H. Yan, X. Lu, C. Chi and J. Xu, *Org. Lett.*, 2014, **16**, 6386–6389.
58 B. B. Patil, Y. Takeda, S. Singh, T. Wang, A. Singh, T. T. Do, S. P. Singh, S. Tokito, A. K. Pandey and P. Sonar, *Sci. Rep.*, 2020, **10**, 19989.
59 B. B. Patil, Y. Takeda, T. T. Do, A. Singh, T. Sekine, S. D. Yambem, S. Tokito, S. P. Singh, A. K. Pandey and P. Sonar, *Phys. Status Solidi*, 2020, **217**, 2000097.
60 Y. Xu, S. Jin, H. Xu, A. Nagai and D. Jiang, *Chem. Soc. Rev.*, 2013, **42**, 8012.
61 M. Rose, *ChemCatChem*, 2014, **6**, 1166–1182.
62 S. Dadashi-Silab, H. Bildirir, R. Dawson, A. Thomas and Y. Yagci, *Macromolecules*, 2014, **47**, 4607–4614.
63 S. Fischer, A. Schimanowitz, R. Dawson, I. Senkovska, S. Kaskel and A. Thomas, *J. Mater. Chem. A*, 2014, **2**, 11825–11829.
64 H. Bildirir, I. Osken, T. Ozturk and A. Thomas, *Chem.–Eur. J.*, 2015, **21**, 9306–9311.
65 H. Bildirir, I. Osken, J. Schmidt, T. Ozturk and A. Thomas, *ChemistrySelect*, 2016, **1**, 748–751.
66 F. Wang, G. Li, D. Qi, I. Hoi-Ka Wong and J. Li, *Polym. Chem.*, 2015, **6**, 459–465.
67 E. B. Sevinis, C. Sahin, M. E. Cinar, M. S. Eroglu and T. Ozturk, *Polym. Eng. Sci.*, 2016, **56**, 1390–1398.
68 B. Ustamehmetoğlu, I. Osken, M. E. Cinar, E. Sezer, E. Karaca and T. Ozturk, *Electrochim. Acta*, 2017, **227**, 435–446.
69 F. Dikcal, S. Topal, M. Unal and T. Ozturk, *Asian J. Org. Chem.*, 2020, **9**, 1309–1317.
70 S. Choi, G. E. Park, J. Shin, H. A. Um, M. J. Cho and D. H. Choi, *Synth. Met.*, 2016, **212**, 167–173.
71 F. Yang, C. Li, J. Zhang, G. Feng, Z. Wei and W. Li, *Org. Electron.*, 2016, **37**, 366–370.
72 J. Yang, B. Xiao, S. W. Heo, K. Tajima, F. Chen and E. Zhou, *ACS Appl. Mater. Interfaces*, 2017, **9**, 44070–44078.
73 H. Tanaka, S. Kawamura, P. Sonar, Y. Shimoi, T. T. Do and T. Takenobu, *Adv. Funct. Mater.*, 2020, **30**, 2000389.
74 L. Ma, S. Dai, X. Zhan, X. Liu and Y. Li, *R. Soc. Open Sci.*, 2018, **5**, 180868.
75 J. Wu, C. Liu, B. Li, F. Gu, L. Zhang, M. Hu, X. Deng, Y. Qiao, Y. Mao, W. Tan, Y. Tian and B. Xu, *ACS Appl. Mater. Interfaces*, 2019, **11**, 26928–26937.
76 I.-B. Kim, Y.-J. Kim, D.-Y. Kim and S.-Y. Jang, *Macromol. Res.*, 2022, **30**, 391–396.
77 S. Topal, O. Savlug Ipek, E. Sezer and T. Ozturk, *Chem. Eng. J.*, 2022, **434**, 133868.
78 O. S. Ipek, S. Topal and T. Ozturk, *Dyes Pigm.*, 2021, **192**, 109458.
79 M. Kaltenbrunner, M. S. White, E. D. Głowacki, T. Sekitani, T. Someya, N. S. Sariciftci and S. Bauer, *Nat. Commun.*, 2012, **3**, 770.
80 M. Ans, F. Manzoor, K. Ayub, F. Nawaz and J. Iqbal, *J. Mol. Model.*, 2019, **25**, 222.
81 W. Liu, F. Wang and L. Li, *J. Theor. Comput. Chem.*, 2003, **2**, 257–272.
82 Q. Zhang, B. Kan, F. Liu, G. Long, X. Wan, X. Chen, Y. Zuo, W. Ni, H. Zhang, M. Li, Z. Hu, F. Huang, Y. Cao, Z. Liang, M. Zhang, T. P. Russell and Y. Chen, *Nat. Photonics*, 2015, **9**, 35–41.
83 J. Zhou, Y. Zuo, X. Wan, G. Long, Q. Zhang, W. Ni, Y. Liu, Z. Li, G. He, C. Li, B. Kan, M. Li and Y. Chen, *J. Am. Chem. Soc.*, 2013, **135**, 8484–8487.
84 H. C. Lim, J.-J. Kim, J. Jang and J.-I. Hong, *New J. Chem.*, 2018, **42**, 11458–11464.
85 H. C. Lim, M.-S. Choi, S. Chae, H. J. Kim, J.-J. Kim and J.-I. Hong, *J. Mater. Chem. C*, 2020, **8**, 11145–11152.
86 M. Iyoda and H. Shimizu, *Chem. Soc. Rev.*, 2015, **44**, 6411–6424.
87 M. Hasegawa, R. Inoue and Y. Mazaki, *Synlett*, 2016, **27**, 2407–2415.
88 M. Hasegawa, K. Takahashi, R. Inoue, S. Haga and Y. Mazaki, *Chem.–Asian J.*, 2019, **14**, 1647–1650.
89 Y. Nishiyama, K. Tokunaga and N. Sonoda, *Org. Lett.*, 1999, **1**, 1725–1727.
90 T. Yamamoto, T. Nishimura, T. Mori, E. Miyazaki, I. Osaka and K. Takimiya, *Org. Lett.*, 2012, **14**, 4914–4917.
91 J. Shi, L. Xu, Y. Li, M. Jia, Y. Kan and H. Wang, *Org. Electron.*, 2013, **14**, 934–941.
92 J.-D. Huang, S.-H. Wen and K.-L. Han, *Chem.–Asian J.*, 2012, **7**, 1032–1040.
93 C.-Z. Wang, J.-H. Do, T. Akther, X. Feng, T. Matsumoto, J. Tanaka, C. Redshaw and T. Yamato, *J. Lumin.*, 2017, **188**, 388–393.
94 Y. S. Yang, T. Yasuda, H. Kakizoe, H. Mieno, H. Kino, Y. Tateyama and C. Adachi, *Chem. Commun.*, 2013, **49**, 6483.
95 T. Ma, H. Wang, K. Zhao, B. Wang, P. Hu, H. Monobe, B. Heinrich and B. Donnio, *ChemPlusChem*, 2019, **84**, 1439–1448.
96 J. Vollbrecht, P. Oechsle, A. Stepen, F. Hoffmann, J. Paradies, T. Meyers, U. Hilleringmann, J. Schmidtke and H. Kitzerow, *Org. Electron.*, 2018, **61**, 266–275.
97 D. Ho, M. Jeon, H. Kim, O. Gidron, C. Kim and S. Seo, *Org. Electron.*, 2018, **52**, 356–363.
98 K. He, S. Zhou, W. Li, H. Tian, Q. Tang, J. Zhang, D. Yan, Y. Geng and F. Wang, *J. Mater. Chem. C*, 2019, **7**, 3656–3664.
99 T. Xia, C. Li, H. S. Ryu, X. Sun, H. Y. Woo and Y. Sun, *Sol. RRL*, 2020, **4**, 2000061.
100 S. Park, Y. Jang, E. Choi, D. Ho, W. Chae, T. Earmme, C. Kim and S. Seo, *Thin Solid Films*, 2022, **745**, 139112.
101 E. Choi, Y. Jang, D. Ho, W. Chae, T. Earmme, C. Kim and S. Seo, *Coatings*, 2021, **11**, 1222.
102 S. Saito and A. Osuka, *Angew. Chem., Int. Ed.*, 2011, **50**, 4342–4373.
103 M. Stępień, N. Sprutta and L. Latos-Grażyński, *Angew. Chem., Int. Ed.*, 2011, **50**, 4288–4340.

104 S. Dash, A. Ghosh and T. K. Chandrashekar, *J. Porphyr. Phthalocyanines*, 2020, **24**, 98–104.
105 T. K. Chandrashekar, V. Prabhuraja, S. Gokulnath, R. Sabarinathan and A. Srinivasan, *Chem. Commun.*, 2010, **46**, 5915–5917.
106 A. Ghosh, A. Srinivasan, C. H. Suresh and T. K. Chandrashekar, *Chem.–Eur. J.*, 2016, **22**, 11152–11155.
107 W.-Y. Cha, T. Kim, A. Ghosh, Z. Zhang, X.-S. Ke, R. Ali, V. M. Lynch, J. Jung, W. Kim, S. Lee, S. Fukuzumi, J. S. Park, J. L. Sessler, T. K. Chandrashekar and D. Kim, *Nat. Chem.*, 2017, **9**, 1243–1248.
108 W.-Y. Cha, A. Ahn, T. Kim, J. Oh, R. Ali, J. S. Park and D. Kim, *Chem. Commun.*, 2019, **55**, 8301–8304.
109 M. Macchione, N. Chuard, N. Sakai and S. Matile, *ChemPlusChem*, 2017, **82**, 1062–1066.
110 M. Macchione, A. Goujon, K. Strakova, H. V. Humeniuk, G. Licari, E. Tajkhorshid, N. Sakai and S. Matile, *Angew. Chem., Int. Ed.*, 2019, **131**, 15899–15903.
111 X. Zhang, N. Sakai and S. Matile, *ChemistryOpen*, 2020, **9**, 18–22.
112 J. García-Calvo, J. López-Andarias, N. Sakai and S. Matile, *Helv. Chim. Acta*, 2022, **105**, e202100238.
113 S. N. Afraj, C. Lin, A. Velusamy, C. Cho, H. Liu, J. Chen, G. Lee, J. Fu, J. Ni, S. Tung, S. Yau, C. Liu, M. Chen and A. Facchetti, *Adv. Funct. Mater.*, 2022, **32**, 2200880.
114 P. S. Gangadhar, S. Gonuguntla, S. Madanaboina, N. Islavath, U. Pal and L. Giribabu, *J. Photochem. Photobiol., A*, 2020, **392**, 112408.
115 Y. Cai, L. Du, K. Samedov, X. Gu, F. Qi, H. H. Y. Sung, B. O. Patrick, Z. Yan, X. Jiang, H. Zhang, J. W. Y. Lam, I. D. Williams, D. Lee Phillips, A. Qin and B. Z. Tang, *Chem. Sci.*, 2018, **9**, 4662–4670.
116 R. Isci, E. Tekin, K. Kaya, S. Piravadili Mucur, S. F. Gorkem and T. Ozturk, *J. Mater. Chem. C*, 2020, **8**, 7908–7915.
117 S. Vegiraju, X.-L. Luo, L.-H. Li, S. N. Afraj, C. Lee, D. Zheng, H.-C. Hsieh, C.-C. Lin, S.-H. Hong, H.-C. Tsai, G.-H. Lee, S.-H. Tung, C.-L. Liu, M.-C. Chen and A. Facchetti, *Chem. Mater.*, 2020, **32**, 1422–1429.
118 S. Vegiraju, D.-Y. Huang, P. Priyanka, Y.-S. Li, X.-L. Luo, S.-H. Hong, J.-S. Ni, S.-H. Tung, C.-L. Wang, W.-C. Lien, S. L. Yau, C.-L. Liu and M.-C. Chen, *Chem. Commun.*, 2017, **53**, 5898–5901.
119 C.-C. Lin, S. N. Afraj, A. Velusamy, P.-C. Yu, C.-H. Cho, J. Chen, Y.-H. Li, G.-H. Lee, S.-H. Tung, C.-L. Liu, M.-C. Chen and A. Facchetti, *ACS Nano*, 2021, **15**, 727–738.
120 P.-O. Schwartz, S. Förtsch, A. Vogt, E. Mena-Osteritz and P. Bäuerle, *Beilstein J. Org. Chem.*, 2019, **15**, 1379–1393.
121 C. Zhang, Z. Ma, G. Wang, C. Li and H. Wang, *Org. Chem. Front.*, 2020, **7**, 3926–3934.
122 Z. Lamprecht, F. P. Malan, I. Fernández, S. Lotz and D. I. Bezuidenhout, *Dalton Trans.*, 2020, **49**, 15339–15354.
123 J. L. Brusso, O. P. Clements, R. C. Haddon, M. E. Itkis, A. A. Leitch, R. T. Oakley, R. W. Reed and J. F. Richardson, *J. Am. Chem. Soc.*, 2004, **126**, 8256–8265.
124 H. Matsuzaki, W. Fujita, K. Awaga and H. Okamoto, *Phys. Rev. Lett.*, 2003, **91**, 017403.
125 H. Zhang, H. Dong, Y. Li, W. Jiang, Y. Zhen, L. Jiang, Z. Wang, W. Chen, A. Wittmann and W. Hu, *Adv. Mater.*, 2016, **28**, 7466–7471.